-修士論文-

Coupling Coefficient Estimation for Wireless Power Transfer via Magnetic Resonant Coupling Using Information from Either Side of the System

（磁界共振結合を用いたワイヤレス電力伝送のための一次側もしくは二次側からの情報による結合係数推定）

平成25年2月6日(水)提出

指導教員:　堀洋一教授

東京大学大学院

工学系研究科電気系工学専攻

堀・藤本研究室

37-116509　JIWARIYAVEJ　VISSUTA

（ジワリヤウェート　ウィツター）

ABSTRACT

Wireless power transfer via magnetic resonant coupling method has open new possibility to electric vehicle (EVs) system. One is that it allows the wireless charging system of moving vehicles, using charging lanes. However, although the efficiency of power transmission is still relatively high, the efficiency still depends on the displacement of antennas. There have been several researches on methods to maintain power transmission at highest efficiency, such as impedance matching system or using control algorithm. However, in such systems, information on system parameter especially coupling coefficients is needed and in charging lane system, such information is unlikely to be obtainable without communication system which will add complexity to the system. Therefore it has come into attention that parameter estimation is the crucial factor to implement the charging lane system.

In this study, coupling coefficient (k) estimation without using any communications between sending and receiving sides is proposed for wireless power transfer via magnetic resonant coupling. Theoretical estimation equations for k is proposed for both estimation from transmitting side and from receiving side, for both the system with single receiver and the system with multiple receivers. Coupling coefficient estimation system implementation is done for estimation from the receiving side using DC/DC converter. The estimation scheme based on statistical method such as recursive least square method taking errors caused by measurement error and hardware imperfection into consideration was studied to improve k estimation accuracy in actual system implementation.

Contents

1 Introduction **1**
- 1.1 EV Charging Technology . . . 2
  - 1.1.1 Conductive Coupling Charging System . . . 2
  - 1.1.2 Contactless Charging System . . . 4
- 1.2 Methods of Improvement for Wireless Power Transfer . . . 10
- 1.3 Literature Review on k parameter estimation . . . 12
  - 1.3.1 Coupling factor estimation for efficiency optimization on wireless power transfer . . . 12
  - 1.3.2 Pinpoint Wireless Power Transformation System using Reflection Coefficient in Magnetic Resonance Coupling . . . 12
  - 1.3.3 A Primary Side Controller for Inductive Power Transfer Systems . . . 14
- 1.4 Proposed Study . . . 14

2 Equations for k Estimation **16**
- 2.1 Equivalent Circuit . . . 16
- 2.2 Estimation Equation from Transmitting Side . . . 18
  - 2.2.1 With single receiver . . . 19
  - 2.2.2 With multiple receivers . . . 20
- 2.3 Estimation Equation from Receiving Side . . . 21
  - 2.3.1 With single receiver . . . 22
  - 2.3.2 With multiple receivers . . . 23
- 2.4 Simulation and Experimental Results . . . 24
  - 2.4.1 Estimation Result from Transmitting Side with Single Receiver (Reference Value) . . . 25
  - 2.4.2 Estimation Result from Transmitting Side with Multiple Receivers . 25
  - 2.4.3 Estimation Result from Receiving Side . . . 26

3 System Implementation using DC/DC **30**
- 3.1 Concept of DC/DC Converter . . . 30
- 3.2 System simulation in MATLAB/SimPowerSystem . . . 31
  - 3.2.1 Simulation Setup . . . 31
  - 3.2.2 Simulation Result . . . 33
- 3.3 Experimental System . . . 34
  - 3.3.1 Possible Causes of Estimation Error . . . 37

4 k Estimation Error Reduction using Recursive Least Square Method 42
4.1 Least Square Estimation 42
4.2 Recursive Least Square 46

5 Conclusion 51

A Effect of Obstacles to Power Transfer Efficiency 53
A.1 Effect from Mobile Robot 53
A.2 Effect from Bentonite 53

Publications 60

Acknowledgements 61

List of Tables

1.1 Characteristics of contactless power transfer method 11

2.1 Antenna Parameters 24

3.1 Comparison between Buck, Boost, Buck-Boost DC/DC Converter 31

List of Figures

1.1 Shaghai capacitor bus infrastructurer . . . 3
1.2 DC Fast Charging Station . . . 4
1.3 Concept of EV charging system via microwave road . . . 5
1.4 Concept of EV charging system via power beam . . . 6
1.5 Diagram for magnetic induction method . . . 7
1.6 On-Line Electric Vehicle (OLEV) System by KAIST . . . 8
1.7 Efficiency comparison between the proposed WiTricity system and a typical magnetic coupling system . . . 9
1.8 Power transfer characteristics due to misalignment . . . 9
1.9 Capacitive coupling charging system . . . 10
1.10 k estimation system diagram using data transmission . . . 12
1.11 Concept of pinpoint wireless power transfer . . . 13
1.12 Flow chart of pinpoint wireless power transfer system . . . 13
1.13 Wireless power transfer system with a primary sense controller . . . 14

2.1 T-type equivalent circuit for wireless power transfer . . . 17
2.2 Equivalent circuit for system with multiple receivers . . . 20
2.3 V_2characteristics . . . 22
2.4 900kHz antenna . . . 24
2.5 Wireless power transfer system setup . . . 25
2.6 Reference Value . . . 26
2.7 Simulation result for k_{12} and k_{13} estimation from transmitting side . . . 27
2.8 Experiment result for k_{12} and k_{13} estimation from transmitting side using frequency sweep . . . 28
2.9 Simulation result for k_{12} estimation from receiving side . . . 29
2.10 Experiment result for k_{12} estimation from receiving side using impedance sweep . . . 29

3.1 Schematics of Buck (left), Boost (middle), Buck-Boost (right) converters . 31
3.2 System Simulation in Simulink . . . 32
3.3 Response of system simulation when using D=0.3 and D=0.7 to estimate k_{12} 34
3.4 Simulation result of k estimation system using ideal DC/DC converter . . . 35
3.5 Experimental system diagram . . . 36
3.6 Experimental system built on test board . . . 36
3.7 Experimental setup with k estimating system using DC/DC converter . . . 37
3.8 Experimental result of k estimation system using experimental system . . . 38

3.9 Experimental setup for moving load 39
3.10 Diode rectifier characteristics 40
3.11 Buck-boost converter characteristics 41

4.1 k estimation result using VNA calibration 43
4.2 k estimation result with least square method for single receiver 47
4.3 k estimation result with least square method for two receivers 48
4.4 Block diagram of recursive least square method 49

A.1 Power transfer efficiency due to various configurations of experimental system 54
A.2 One possible configuration for experimental setup to avoid effect from mobile robot 54
A.3 Experimental setup with bentonite 55
A.4 Efficiency comparison 56

Chapter 1

Introduction

Recently, the development of electric vehicles (EVs) has been gaining more attentions from both consumers and research community as EVs are potential alternatives to traditional conbustion engine cars. However, despite tremendous effort put in improving EVs, the main drawback of EVs which is in battery storage still remains. Currently used batteries have relatively low energy density; hence EVs cannot travel across long distance unless the amount of battery is increased. But by doing so, the EV will become heavier which is not desirable. The effort to overcome the limited travelling distance of EVs started as early as 1896.

The first attempt, although not by charging station, is proposed and put into practice by Hartford Electric Light Company as an exchangeable battery service [1]. In modern days, some battery exchange station has also been built and tested in operation. However, the infrastructure takes up relatively large space and therefore not very practical. Therefore, researchers have paid more attention to development and improvement of EVs charging systems.

1.1 EV Charging Technology

Mainly, there are two types of charging systems: conductive coupling system and contactless charging system [2]. Conductive coupling are traditional wired charger where electricity is transmitted via direct ohmic contact between power source and the load. In contrast, in contactless charging system, as the name suggested, there is no direct contact between the source and the load. There are several methods of transmitting power wirelessly listed as following: microwave transmission, magnetic induction, magnetic resonance coupling and capacitive coupling.

1.1.1 Conductive Coupling Charging System

Conductive coupling charging system uses the conventional conductive contact to transmit power. In other word, electricity is transferred through wire and therefore the user has to plug in the charging cable from source to the vehicle. Power source can be either from home outlet or charging station. Because power transmission is accomplished through conductive connection, power loss is only caused by ohmic loss, and therefore transmitting efficiency is high. However, the problem with battery charging system is charging time. Typical battery equipped in the EVs could take 8-12 hours to fully charge. Instead of waiting for a long charging time, the idea of fast charging system, which let vehicle be recharged enough to travel between charging spots using short charging time, has become attractive. Two main trends of development is, first, change energy storage type from battery to capacitor and, second, using DC fast charger.

Capacitor Storage

In contrast to battery, although having smaller capacity, capacitor has high rate of charge and discharge time, and therefore significantly reduces charging time. One example that utilizes such characteristics of capacitor is Shanghai SUNWIN capacitor bus [3]. The bus

Figure 1.1: Shaghai capacitor bus infrastructurer

is equipped with super capacitor and a railway-style pantograph so that the capacitor can be recharged from the charging system placed at the bus station while the bus stops to take the passengers. The infrastructure of such bus system is shown in Fig. 1.1. Bus capacitor is charged with 320-600V DC system. With charging time of 30-80 seconds, the bus can run over the distance of 3-6 km which is enough to go between stations.

DC Fast Charger

DC fast charger has become more popular due to its benefit [4]. Fast chargers are known to be more efficient than conventional chargers and less overcharge occurs, hence increase battery efficiency and life-cycle. Charging schemes can be done in many ways.

To universalize fast charging system, one of the most used standards is CHAdeMO (Charge de Move) standard, started by collaboration of several car manufacturers [6]. Examples of charging stations are shown in Figure 1.2. Currently there are almost one thousand charging stations around the world while 747 stations are located in Japan.

Despite such high efficiency and improvement in wired charging system, there are still some disadvantages that might hold users back from adopting EVs technologies. Manually charging EVs could be inconvenient. The charging system could take up a lot of space in household. Moreover, possible hazard from electric shock could occur while handling with the charger. Due to such reason, contactless charging systems have become a potential technology that could lead to expansion of EVs.

Figure 1.2: DC Fast Charging Station

1.1.2 Contactless Charging System

To overcome disadvantages of wired charging systems, much effort has been put into developing contactless power transmission system. There are several technologies available for wireless transmission: microwave transmission, magnetic induction, magnetic resonance coupling and capacitive coupling. In this section, EV charging system utilizing each method, including its characteristics, advantages, drawbacks, possible improvement, will be described.

Microwave Transmission

Microwave power transmission utilized microwaves to transfer power through space. This method is proposed due to its ability to transfer power across long distance of several kilometers. There is also a large range of usable transmitting frequency. However, two main limitations of this method of transmission are that it requires direct line of sight with no obstacle In this section, two type of dynamic charging systems proposed will be introduced.

1. Dynamic charging system via microwave road [7]

   In this system, rectenna array are equipped underneath the vehicle. On the road side, waveguide slot antennas and optical sensors are placed on the road so that when

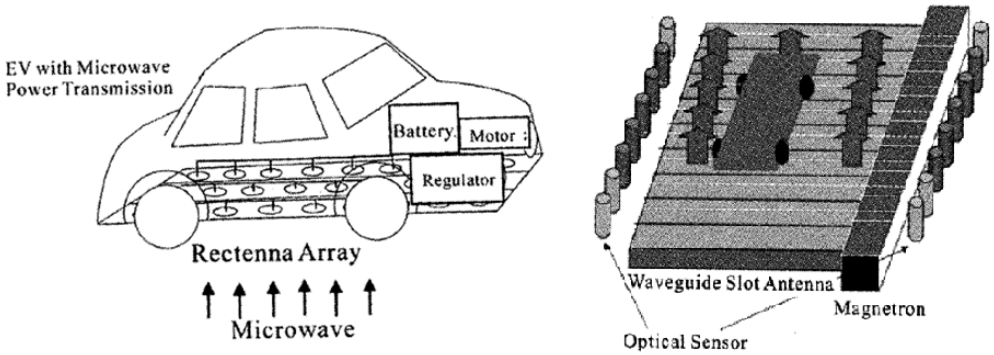

(a) EV charging system via microwave (b)Microwave road in final system

Figure 1.3: Concept of EV charging system via microwave road

the vehicle is passing through the lane, powered will be transmitted directly to the vehicle above the lane. The concept of this system configuration is shown in Figure 1.3.

Using the prototype system, power transfer efficiency is measured in the experiment. Efficiency of conversion from DC power to radio frequency (RF) wave is 72%, of wave guide antenna is 58%, radiation loss reduce efficiency for another 67% and conversion from RF back to DC has efficiency of 55%. Such configuration results in the total efficiency of power transmission as low as 15% mainly caused by conversion between DC and RF.

2. Microwave transmission via guided power beam [8]

   In contrast to the aforementioned system configuration for microwave transmission, in this system, power will be transferred to the antenna equipped on top of the vehicle from power beam transmitter. System components are shown in Figure 1.4(a). This method, although has not been actually implemented, were aiming to utilized one of the advantage of microwave transmission, which is the power beam can be steered electrically, without moving mechanisms. Figure 1.4(b) shows the intended dynamic charging system. Via communication beam, the position of the vehicle should be determined and the closest power post will transmit the power to the vehicle via

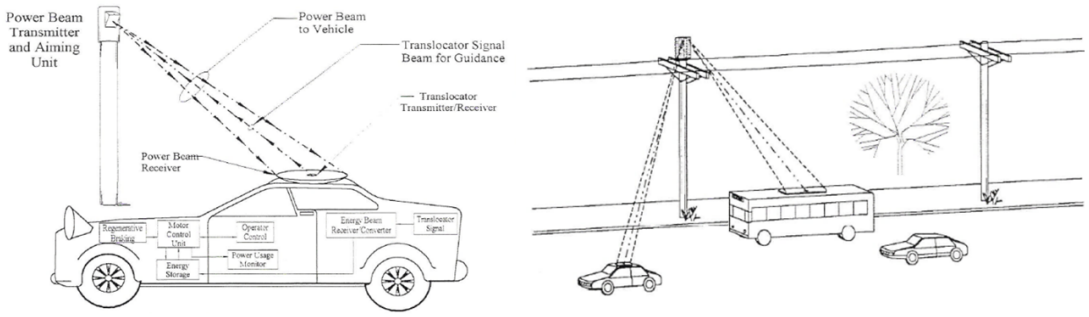

(a) EV for power beam charging system (b) Wireless power beam network

Figure 1.4: Concept of EV charging system via power beam

power beam. Once the vehicle has moved out of the transmitting range, the next transmission post will take over and repeat the same process for transmission.

Magnetic Induction

Magnetic induction method composed of the primary coil and secondary coil which function as transmitter and receiver respectively. In contrast to microwave transmission, obstacle between coils will not completely prevent transmission to occur in magnetic induction method, although transmission efficiency might be decreased. Usually, there will be an inverter on the transmitting side to modify the wave sent from source to the desired frequency and a rectifier on the receiving side to convert AC to DC in order to charge the battery. A simple structure of circuit for wireless charger with magnetic induction method is shown in Figure 1.5(a).

From the equivalent circuit shown in Figure 1.5(b), voltage V_1 excites the primary coil which cause magnetisc flux to link to the secondary coil, and therefore generate voltage V_2 in the receiver [9].

Let $I_1, I_2, L_1, L_2, R_1, R_2$ be current, inductance and internal resistance of transmitter and receiver circuit respectively, and M be mutual inductance between transmitting and receiving coils, the relation between the coil voltage and current can be expressed as following:

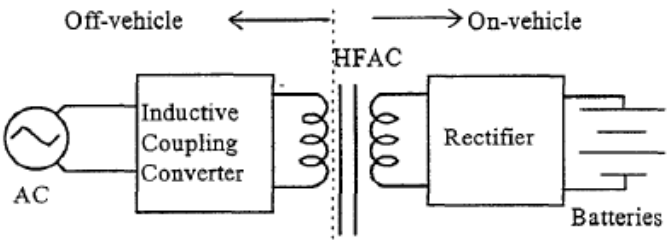

(a) Simple block diagram for charging circuit

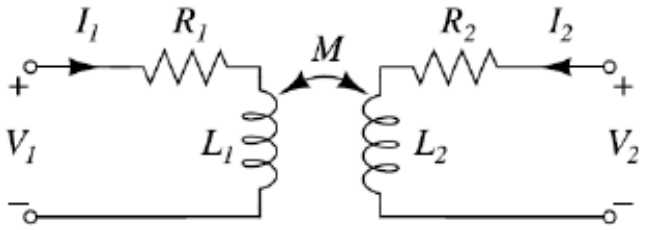

(b) Equivalent circuit for magnetic induction method

Figure 1.5: Diagram for magnetic induction method

$$\begin{bmatrix} V_1 \\ V_2 \end{bmatrix} = \begin{bmatrix} R_1 + j\omega L_1 & j\omega M \\ j\omega M & R_2 + j\omega L_2 \end{bmatrix} \begin{bmatrix} I_1 \\ I_2 \end{bmatrix} \tag{1.1}$$

Without any tuning or compensation, the transmitting efficiency is usually not very high.

Attempting to utilize the advantage of wireless characteristics of magnetic induction transmission method, a dynamic charging system by magnetic induction method has been proposed since 1990 as a roadway powered electric vehicle (RPEV) system. The concept is to bury a rail of transmitting coil underneath the road surface, from where a vehicle can receive the power while running above.

In 2009, such dynamic charging system called On-Line Electric Vehicle (OLEV), shown in Figure 1.6, has been implemented by KAIST [11]. The air gap between transmitting and receiving coil in the last generation OLEV is 17cm where 72% efficiency is achieved. Although with compensation, transmission gap will not affect the efficiency that much, the transfer efficiency of magnetic induction method is severely subjected to positioning mis-

Figure 1.6: On-Line Electric Vehicle (OLEV) System by KAIST

alignment of the coils. Therefore, in order for OLEV to operate properly, position control system is equipped so that the vehicle will not diverge from the rail more than 3mm.

Magnetic Resonance Coupling

In 2007, the MIT WiTricity opened the experiment on wireless power transfer via strongly coupled magnetic resonance to public [12]. Based on similar principal as magnetic induction method, however, the transmitting and receiving coil are designed to have the same self-resonant frequency. Therefore, even before adding any compensation into the circuit, the system always operates in a way that transmitting and receiving circuits are in resonant. By doing so, the energy efficiency of power transfer increase significantly compared to the traditional magnetic induction method [13]. Figure 1.7 shows the efficiency comparison between magnetic induction method and recently released magnetic resonance coupling method. Efficiency with respect to several alignments of transmitter and receiver coils is investigated in [14]. By designing the self-resonant frequency of the coil to be the same as operating frequency of power source, power can be transferred with high efficiency even at the distance almost equal to the size of antenna.

One great advantage of transmission by magnetic resonance coupling method is that power transfer is robust to positional misalignment of transmitting and receiving antennas. Figure 1.8 is experimental setup and result showing that transmission efficiency does not

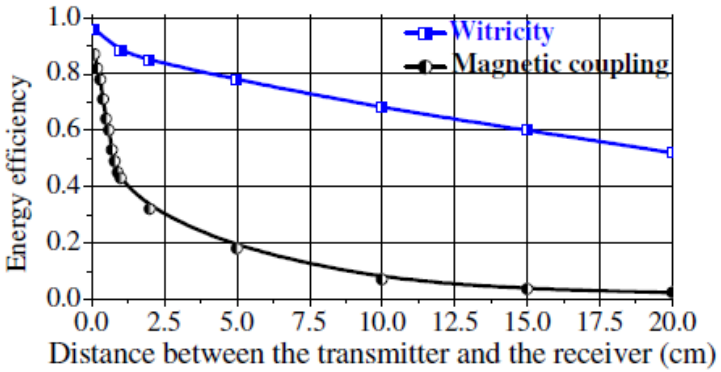

Figure 1.7: Efficiency comparison between the proposed WiTricity system and a typical magnetic coupling system

(a) Experimental setup to investigate transmission characteristics vs. antenna misalignment

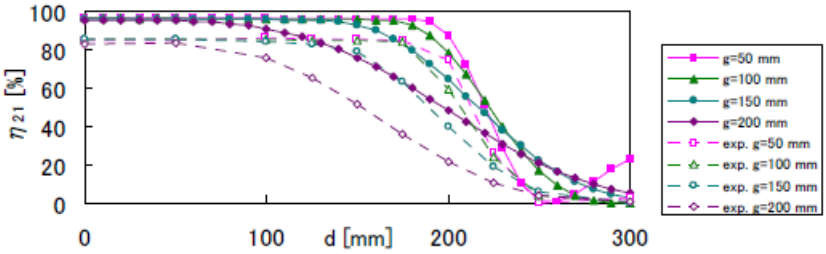

(b) Transmission efficiency vs. misalignment

Figure 1.8: Power transfer characteristics due to misalignment

drop that much for a wide range of antenna misalignment [14].

Capacitive Coupling

Capacitive coupling is power transmission by means of capacitance between two points in a circuit, which can be done by placing a capacitor in series into the path of power transmission. In [18], power transmission via capacitor composed of a steel belt and a

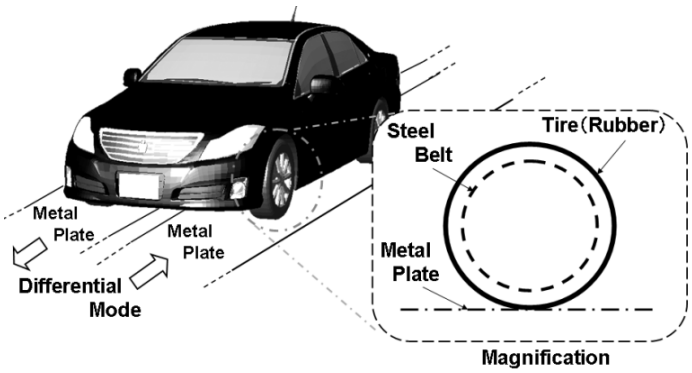

(a) Capacitive tire system diagram

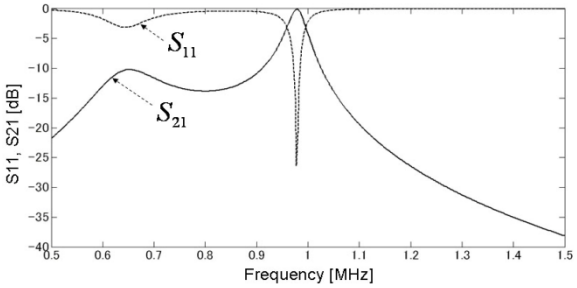

(b) Transmitting coefficient vs. operating frequency

Figure 1.9: Capacitive coupling charging system

metal plate attached to the road surface is proposed. The system diagram is shown in Figure 1.9(a), and the efficiency with respect to operating frequency is shown in Figure 1.9(b).

For the purpose of implementing dynamic charging system, which lets vehicles recharge while moving and hence allows EVs to run for virtually unlimited range, magnetic resoncnce coupling method seems to have the most potential. The reason is that this method can transfer power with high efficiency across relatively long distance while being robust to antennas' positional misalignment without the need of complicated compensation.

1.2 Methods of Improvement for Wireless Power Transfer

Despite theoretically high efficiency, there are some events where the system is out of resonant due to some characteristics of this method or due to some imprecision in system construction, compensation is used to improve transmission efficiency even further.

Table 1.1: Characteristics of contactless power transfer method

Method	Microwave	Magnetic Induction	Magnetic Resonance Coupling	Capacitive Coupling
Frequency	GHz/THz	kHz	kHz/MHz	kHz/MHz
Transmission Range	Very long (km)	Short (<10cm)	Mid-range (<10m)	Mid-range (10-40cm)
Efficiency	< 54%	> 90%	> 90%	< 80%
Advantage	Transmission direction can be steered electrically	Low cost in construction	Robust to positioning misalighment	Simple to manufacture
Disadvantage	Low efficiency. Require direct line of signt between source and target	Efficiency is strongly subject to antenna's misalignment	Efficiency is subject to antenna's self-resonant frequency	Subject to tire slip

1. Impedance Matching Method [15]

   LC circuit is inserted to modify input impedance. The highest efficiency occurs when the input impedance equals to complex conjugate of source impedance.

2. Frequency Tracking [16]

   This method of transmission operates on the principal that self-resonant frequency of both coils and frequency of power source are the same. Due to imprecision in system construction, some component in the system might be out of resonant, and for such scenario, a control system to adjust the receiver's frequency will be inserted to change the receiver characteristics to the point with highest efficiency.

However, most of these methods require the knowledge of system parameters, especially coupling coefficient (k). And those that do not, due to the use of search algorithm, are still not fast enough for improving efficiency of moving pick-ups. Therefore it has come into attention that parameter estimation is a crucial factor to make the system of charging lane implementable.

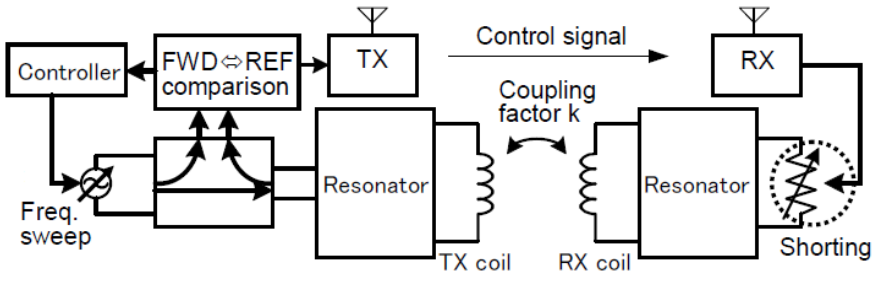

Figure 1.10: k estimation system diagram using data transmission

1.3 Literature Review on k parameter estimation

Although there are many researches regarding wireless power transfer using magnetic resonant coupling method, there are still very few researches that focus on k estimation. This section will introduce some recent work on coupling coefficient estimation method.

1.3.1 Coupling factor estimation for efficiency optimization on wireless power transfer

This study proposed a system for coupling factor estimation shown in Figure 1.10 [19]. For estimation process, the load is shorted for a short period of time to excite the reflection coefficient η_{11} parameter. Such change in η_{11} is then observed from in the source side. By doing so, not only that information from both sides of the wireless power system is necessary for k estimation, but the complexity of the system also increases due to proper timing control of both sides of the system for estimation process.

1.3.2 Pinpoint Wireless Power Transformation System using Reflection Coefficient in Magnetic Resonance Coupling

This study investigated the wireless power transfer system via magnetic resonance coupling method in the scenario that the load appliance approaches the vicinity of more than one transmitting antennas [20]. In order to save energy, power will only be transferred to load

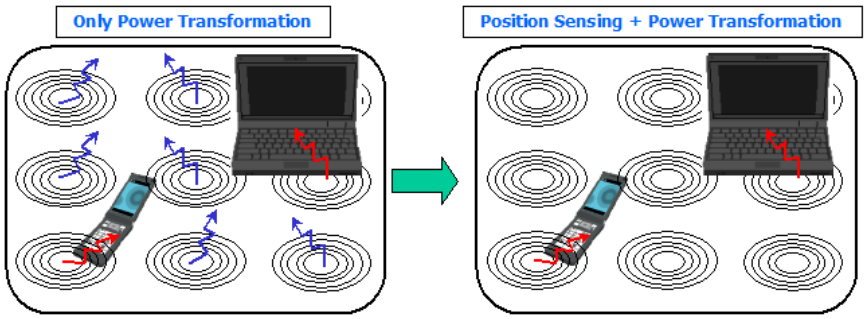

Figure 1.11: Concept of pinpoint wireless power transfer

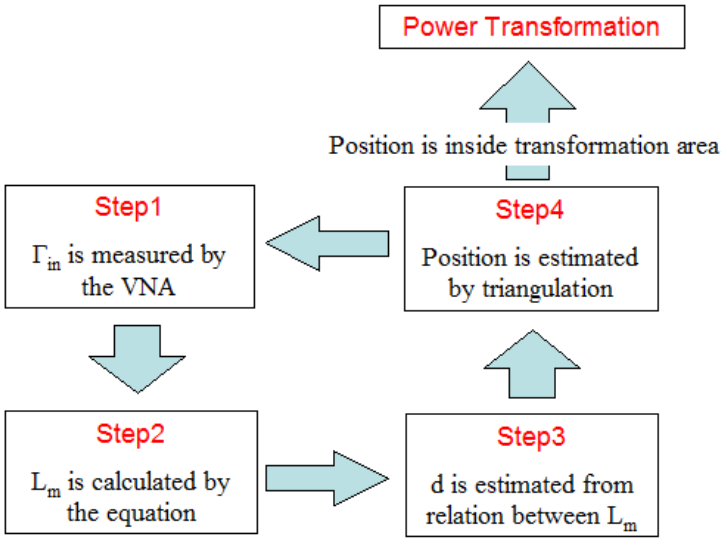

Figure 1.12: Flow chart of pinpoint wireless power transfer system

from the nearest power source or transmitting antenna. The system flow is shown in Figure 1.11.

The distance between receiving antenna or load and transmitting antenna is estimated from reflection coefficient (Γ_{in}) measured by vector network analyzer (VNA). The mutual inductance which is strongly related to the transmission distance is then calculated by equation (1.2).

$$L_m = \frac{z_0}{\omega_0}\sqrt{\frac{1+\Gamma in}{1-\Gamma_{in}}} \tag{1.2}$$

where L_m = mutual inductance [H], Z_0 = source impedance [Ω], ω = system resonance

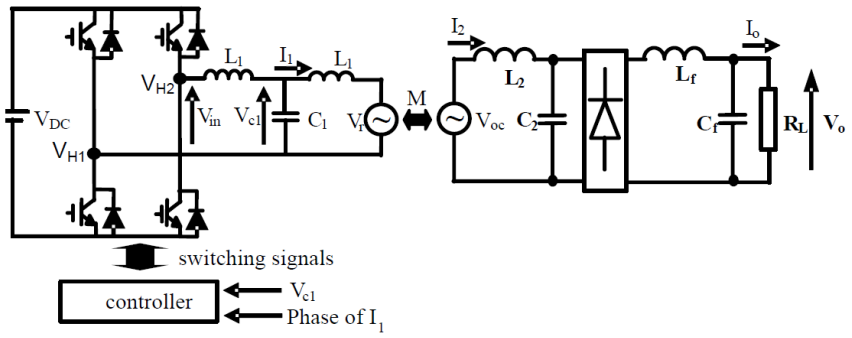

Figure 1.13: Wireless power transfer system with a primary sense controller

angular frequency [rad].

Using this method, the distance can be calculated quite easily and using this calculated distance, charging scheme or rules, such as not to charge unless target is within certain distance from power source, can be set. However, the drawback is that VNA is expensive and the method in this study seems to only work when there is only one receiving antenna.

1.3.3 A Primary Side Controller for Inductive Power Transfer Systems

This study proposed a controller equipped in the transmitting side that can improve wireless power transfer system using mutual coupling value and output voltage estimated by reflected primary voltage [21]. The proposed system is shown in Figure 1.13. The calculation in this method depends heavily on antenna's Q value and this system specific topography. It also does not offer explicit expression for k, therefore this method is not applicable to k estimation in other system.

1.4 Proposed Study

As presented in literature review, there have been several attempts to estimate k. However, those method either requires expensive equipment or relies on relativaly complicated

equation, and they only apply to the case of one receiving antenna. In order to realize EV charging lane system, this study propose estimation equations for both estimation from transmitting side and from receiving side. The estimation equation are in simple form which should relieve calculation load from the controller. Moreover, the proposed equation are also applicable to the case when there are more than one receiving antenna in the system, which equivalent to the situation when there are more than one vehicle entering charging lanes.

Chapter 2

Equations for k Estimation

2.1 Equivalent Circuit

Wireless power transfer system is composed of the transmitting side, or primary system, and the receiving side, or secondary system. In order to transfer power via magnetic resonance coupling method, each side of the system is equipped with a coil-shaped antenna, and the transmitting frequency from power source and self-resonant frequency of both antennas should be designed to be the same. In 2007, when MIT first presented this method of power transmission, coupled mode theory was used to described the phenomenon of energy transfer between antennas[12]. In contrast, in this study, equivalent circuit is used to represent the system in which the antenna's topology is represented as the combination of inductor and capacitor in series with internal resistance[23]. In this way, the system becomes much more comprehensible for electrical engineers and easier for analysis. The equivalent circuit, for configuration with one transmitting antenna and one receiving antenna, is shown in figure 2.1(a).

In this study, wireless power transfer system is modeled by equivalent circuit, in which the antenna is represented as the combination of inductor and capacitor in series with internal resistance[23]. The equivalent circuit, for configuration with one transmitting antenna

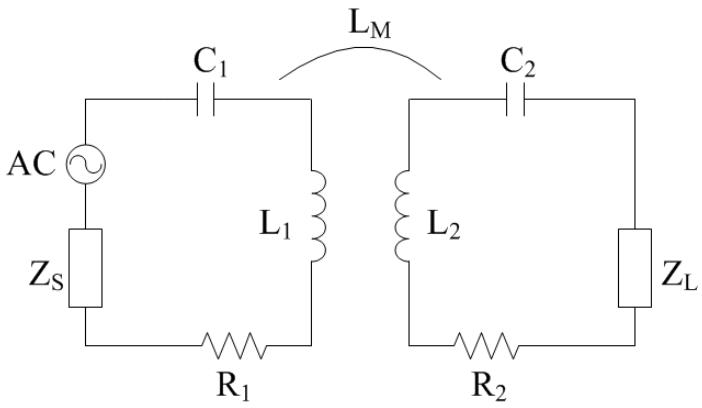

(a) Equivalent circuit

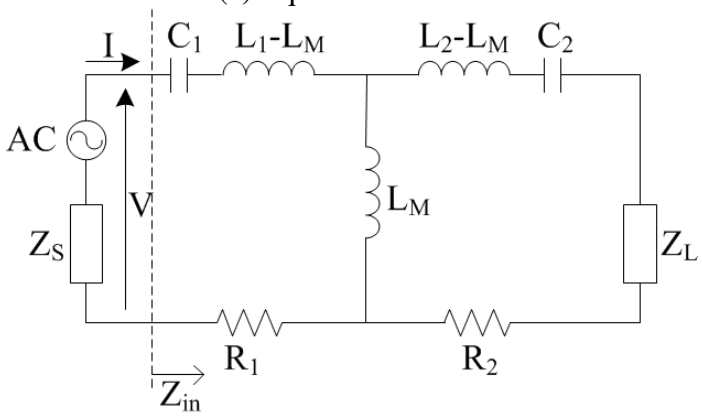

(b) T-type equivalent circuit

Figure 2.1: T-type equivalent circuit for wireless power transfer

and one receiving antenna, is shown in Fig. 2.1(a). This equivalent circuit can also be rewritten as the T-type equivalent circuit illustrated in Fig. 2.1(b).

Parameter L_1, C_1, R_1, L_2, C_2 and R_2 represent the inductance, capacitance, and resistance of transmitting antenna and receiving antenna respectively. Power source impedance is represented by Z_S and load impedance is $Z_L = R_L + jX_L$. Note that, this study will only consider the case when load impedance is purely resistive, in other word, when Z_L does not have an imaginary part. And as mentioned earlier that even though the transmitting side and receiving side of the system are not physically connected, power is transferred with electromagnetic couplings which can be represented as mutual inductance L_m. L_m is the main factor that decides how much power is transferred from the transmitting side to the receiving side, and is also the parameter of interest in this study.

The equivalent circuit in figure 2.1(a) can also be rewritten as the T-type equivalent circuit illustrated in figure 2.1(b). From this equivalent circuit, V_1, I_1 and V_2, I_2 are defined as voltage across and current going through power source and load respectively, immediately before the transmitting antenna, with ϕ as phase different between V_1 and I_1. And lastly, Z_{in} is defined as the equivalent input impedance when looking from power source.

Estimation of coupling coefficient can be done either using only information from source side or only information from load side, depending on the application. In the next two sections, estimation equations will be presented.

2.2 Estimation Equation from Transmitting Side

In this section, estimation equation using only information from source side will be presented. The advantage of estimating coupling coefficient from source side is that, in the case of multiple EVs or receivers having entered the charging system, if the coupling coefficients between transmitting antenna and each receiving antennas are known, not only charging efficiency can be improved, but how much power to distribute to each EV can also be decided using the method introduced in [24].

Looking from source side, the information we can obtain are V_1, I_1, and ϕ. From these parameters, given $V_1 = |V_1|e^{j(\omega t+\phi)}$ and $I_1 = |I_1|e^{j\omega t}$, another information that can be retrieved is input impedance Z_{in} as shown in equation (2.1) .

$$\begin{aligned} Z_{in} &= \frac{V_1}{I_1} \\ &= \frac{|V_1|e^{j(\omega t+\phi)}}{I_1 = |I_1|e^{j\omega t}} \\ &= \frac{|V_1|}{|I_1|} \\ Z_{in} &= \frac{|V_1|}{|I_1|}(\cos\phi + j\sin\phi) \end{aligned} \tag{2.1}$$

$$\text{where } Re\{Z_{in}\} = \frac{|V_1|}{|I_1|}\cos\phi \text{ and } Im\{Z_{in}\} = \frac{|V_1|}{|I_1|}\sin\phi.$$

This Z_{in} parameter can be calculated regardless of the number of the receivers. Therefore estimation equation from source side will be derived mainly in terms of Z_{in}.

2.2.1 With single receiver

From the equivalent circuit, input impedance, Zin, can be calculated, through several steps of calculating equivalent impedance of circuit elements in series and parallel, and rearranged in terms of antenna parameters and load impedance. The derived relations are shown in the equations (2.2) and (2.3) when $Re\{Z_{in}\}$ and $Im\{Z_{in}\}$ represent real part and imaginary part of Z_{in} and ω is defined as power source's operating frequency respectively.

$$Re\{Z_{in}\} = R_1 + \frac{(\omega L_m)^2(Z_L + R_2)}{(Z_L + R_2)^2 + (Z_{A2})^2} \tag{2.2}$$

$$Im\{Z_{in}\} = Z_{A1} - \frac{(\omega L_m)^2(Z_{A2})}{(Z_L + R_2)^2 + (Z_{A2})^2} \tag{2.3}$$

$$\text{where } Z_{A1} = \omega L_1 - \frac{1}{\omega C_1} \text{ and } Z_{A2} = \omega L_2 - \frac{1}{\omega C_2}.$$

However, considering measurement taking, the reliable value of imaginary part of Z_{in} is quite difficult to obtain since it varies quite drastically relative to slightly shifted frequency point. Therefore it is more practical to use measurement of real part in estimation process. Hence, deriving from (2.2), L_m can be estimated using equation (2.4), assuming load value and antenna parameters are known.

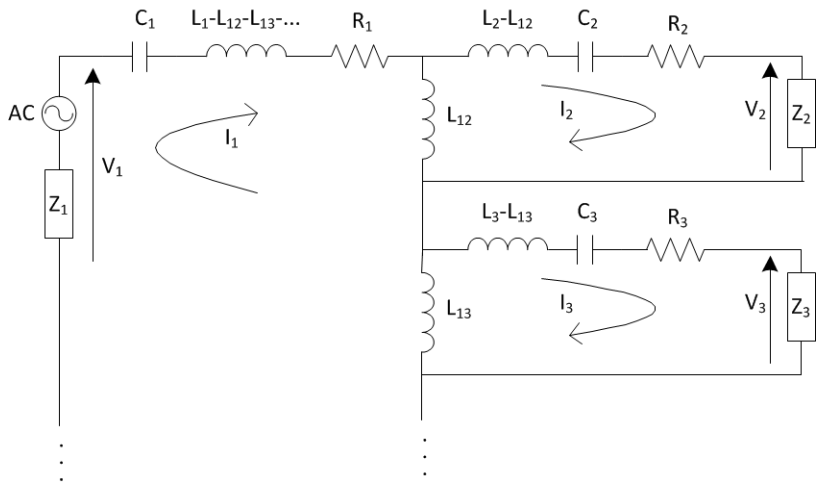

Figure 2.2: Equivalent circuit for system with multiple receivers

$$L_m = \frac{1}{\omega}\sqrt{\frac{[Re\{Z_{in}\} - R_1]\,[(Z_L + R_2)^2 + Z_{A2}^2]}{Z_L + R_2}} \tag{2.4}$$

2.2.2 With multiple receivers

For the case of system with multiple receivers, input impedance can be derived similarly. Equivalent circuit for system with multiple receivers is illustrated in Figure 2.2, where subscription 2 and 3 represent component of load 1 and 2 respectively and so on. In this study, cross-coupling between each load will not be considered due to the fact that this system is aiming for EV charging system, in which receiving antennas in each EVs will have neglegible effect on each other. Z_{in} can be expressed as shown in (2.5).

$$\begin{aligned} Z_{in} &= R_1 + \left(j\omega L_1 + \frac{1}{j\omega C_1}\right) \\ &\quad + \frac{(\omega L_{12})^2}{Z_2 + R_2 + j\omega L_2 + \frac{1}{j\omega C_2}} + \frac{(\omega L_{13})^2}{Z_3 + R_3 + j\omega L_3 + \frac{1}{j\omega C_3}} + \dots \\ &= R_1 + \left(j\omega L_1 + \frac{1}{j\omega C_1}\right) + \sum_{i=2}^{m+1} \frac{(\omega L_{1i})^2}{Z_i + R_i + j\omega L_i + \frac{1}{j\omega C_i}} \end{aligned} \tag{2.5}$$

where m = the number of receiving antennas

In order to solve equation (2.5) for all mutual inductance values, the necessary number of linearly independent equations equals to the number of loads. Controllable parameter in the transmitting side is source frequency. Therefore, once enough information is obtained by performing frequency sweep, mutual inductance values can be calculated by solving equation systems (2.6) expressed below.

$$\begin{bmatrix} Z_{in(1)} \\ Z_{in(1)} \\ \vdots \end{bmatrix} = \begin{bmatrix} P_1 \\ P_2 \\ \vdots \end{bmatrix} + \begin{bmatrix} Q_{11} & Q_{12} & \dots \\ Q_{21} & \ddots & \dots \\ \vdots & \dots & Q_{mm} \end{bmatrix} \begin{bmatrix} L_{12}^2 \\ L_{13}^2 \\ \vdots \end{bmatrix} \tag{2.6}$$

$$\begin{aligned} \text{where } P_j &= R_1 + j\omega_j L_1 + \frac{1}{j\omega_j C_i} \\ Q_{ij} &= \frac{\omega_j^2}{Z_i + R_i + j\omega_j L_i + \frac{1}{j\omega_j C_i}} \\ \text{and } m &= \text{total number of receivers.} \end{aligned}$$

2.3 Estimation Equation from Receiving Side

In this section, estimation equation using only information from load side will be presented. The advantage of estimating coupling coefficient from the load side is when there are more than one receivers in the system. With only one available source, it is more practical to put control from the load side so all loads can match with the one source. Although estimating from load side can only achieve the information of mutual coupling between source and itself but not with other load, the estimation can be done with much less information comparing to source side when the number of loads increases.

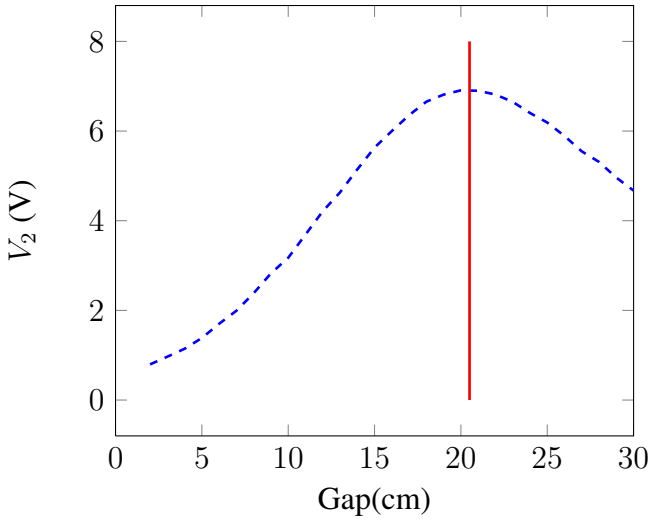

Figure 2.3: V_2characteristics

2.3.1 With single receiver

In the case of single receiver, the relation between mutual coupling L_m and voltage across the load be expressed as shown in equation (2.7) when V_1 is source voltage and V_2 is voltage across load Z_2.

$$L_m = \frac{1}{2\omega}\left[\frac{V_1}{V_2}Z_2 \pm \sqrt{\left(\frac{V_1}{V_2}Z_2\right)^2 + 4R_1(R_2+Z_2)}\right] \tag{2.7}$$

However, due to the characteristics of V_2, which is that it has a peak as illustrated in Figure 2.3, and which sign in equation (2.7) should be used to perform estimation depedns on which side of the peak the system is currently at. Therefore it is not possible to determine L_m with only one set of input sample, which leads to the limitation of estimation from load side using only a single set of information. However, estimation of coupling coefficient from load side can still be performed with the same method as the case of multiple receivers, although additional information is required.

2.3.2 With multiple receivers

In the case of multiple receiving antennas, the estimation is currently done for constant voltage source, assuming source voltage V_1 is known, which a realistic assumption since most power sources are constant voltage source.

$$\frac{V_2}{V_1} = \frac{j\omega L_{12}\left(\frac{Z_2}{R_2+Z_2}\right)}{R_1 + \frac{(\omega L_{12})^2}{R_2+Z_2} + \frac{(\omega L_{13})^2}{R_3+Z_3} + \dots} \tag{2.8}$$

Grouping terms for other antennas together into $Q = R_1 + \frac{(\omega L_{13})^2}{R_3+Z_3} + \dots$, equation (2.8) can be rewritten as follows.

$$\frac{V_2}{V_1} = \frac{j\omega L_{12}\left(\frac{Z_2}{R_2+Z_2}\right)}{\frac{(\omega L_{12})^2}{R_2+Z_2} + Q} \tag{2.9}$$

Currently there are 3 unknowns: V_2, Z_2, which are terms related to the antenna of interest, and Q which contains information of other antennas. However, information from only one instance is not enough to estimate mutual inductance parameter. But if two sets of information, in this case, two voltages across load for different load values, are provided, the estimation can be done by equation (2.10).

$$L_{12} = \frac{V_1}{\omega}\frac{Z_{2a}V_{2b}(R_2+Z_{2b}) - Z_{2b}V_{2a}(R_2+Z_{2a})}{V_{2a}V_{2b}(Z_{2b}-Z_{2a})} \tag{2.10}$$

where V_{2a} = voltage across load when load is Z_{2a}

and V_{2b} = voltage across load when load is Z_{2b}.

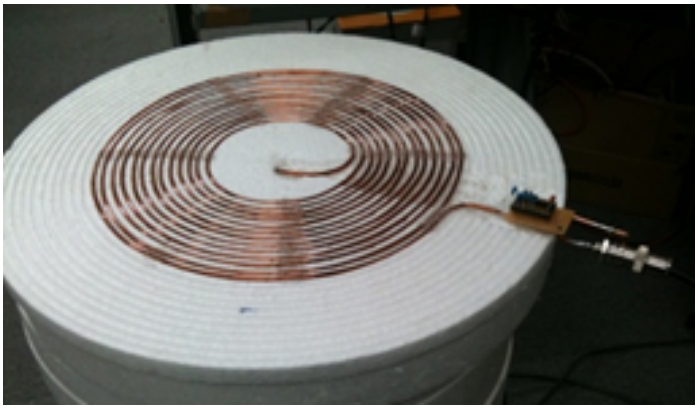

Figure 2.4: 900kHz antenna

Table 2.1: Antenna Parameters

	Resonant Freq. [kHz]	R[Ω]	L[μH]	C[pF]
Transmitting	900.065	1.043	95.562	327.197
Receiving#1	900.821	1.059	97.459	320.289
Receiving#2	902.008	1.058	117.906	268.413

2.4 Simulation and Experimental Results

In order to verify the proposed equation, simple simulation is performed. The antenna which will be used in future experiment is a short-type with self-resonance frequency of approximately 900kHz, shown in Fig. 2.4. The detailed antenna parameters are in TABLE 2.1.

The simulation is performed for the following setup, which is illustrated in Fig. 2.5. The transmitting antenna is fixed in place while the receiving antenna is placed at several distance away from the transmitting antenna. For the case of multiple receivers, the second receiving antenna is placed on the opposite side of the transmitting antenna to avoid cross coupling between the two receivers. Note that, in the actual application of charging lane, two receivers equipped in different vehicles will be too far apart, therefore cross coupling between them should be negligible.

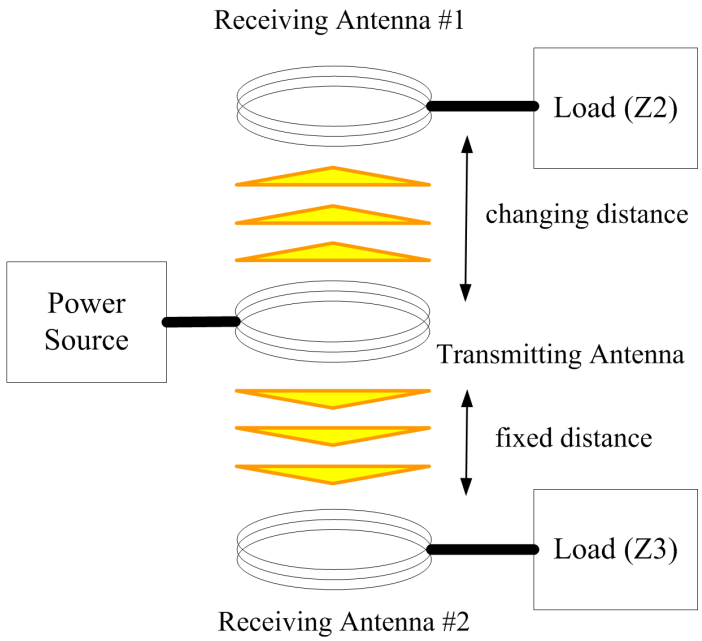

Figure 2.5: Wireless power transfer system setup

2.4.1 Estimation Result from Transmitting Side with Single Receiver (Reference Value)

For this study, since the coupling coefficient or k estimation equation from transmitting side is derived from direct back-calculation, the k value obtained by calculation from this case will be used as a reference value. The calculation is performed for the case when resonant frequency is 900 kHz and load impedance is 50Ω. The expected k value is shown in Fig. 2.6.

2.4.2 Estimation Result from Transmitting Side with Multiple Receivers

For this case, with enough information obtained by frequency sweep, k values between source and each receiver can be estimated. When there are two receivers, information from two frequency points are necessary. Since it is not desireable to make the system too far from the resonant state, the frequencies used in simulation and experiments are 898 kHz, 900 kHz and 902 kHz which is very close to 900 kHz resonant frequency of the system,

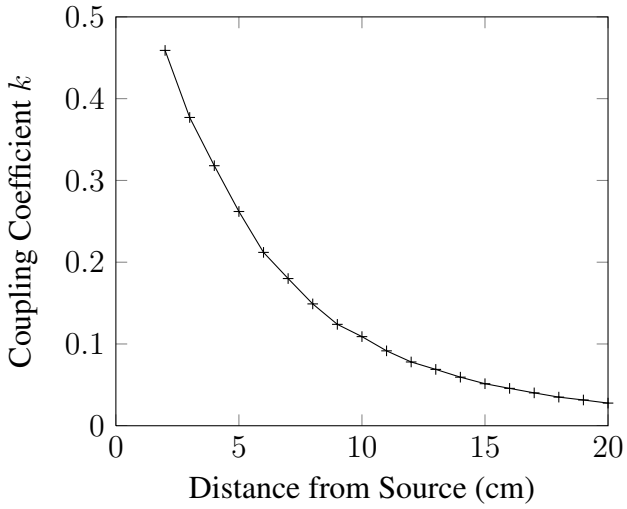

Figure 2.6: Reference Value

whereas load impedance is fixed at 50 Ω. Expected value of k_{12} and k_{13} are calculated in simulation whose result is shown in Fig. 2.7. The plot shows k_{12} and k_{13} versus the distance between transmitting antenna and the first receiving antenna which is moved to several distance. The result of k_{12} matches with reference value while k_{13} is constant as expected since the second receiving antenna is fixed in place. The experimental result is shown in Fig. 2.8. The experimental result, except for the range of extremely short transmitting gap, is mostly consistent with expected value from simulation. The cause of this estimation error for short transmitting gap is due to stray capacitance occured between wires of both antennas. Since the capacitance value is also one parameter in the k estimation equation, such stray capacitance will result in estimation error.

2.4.3 Estimation Result from Receiving Side

Due to the fact that estimation equations are the same whether there are only one or multiple receivers, only estimation result in the case of multiple receivers are presented. More information on receiving side can be gained by changing load, or impedance sweep. The impedance values used in simulation and experiment are 25Ω, 50Ω and 100Ω, whereas

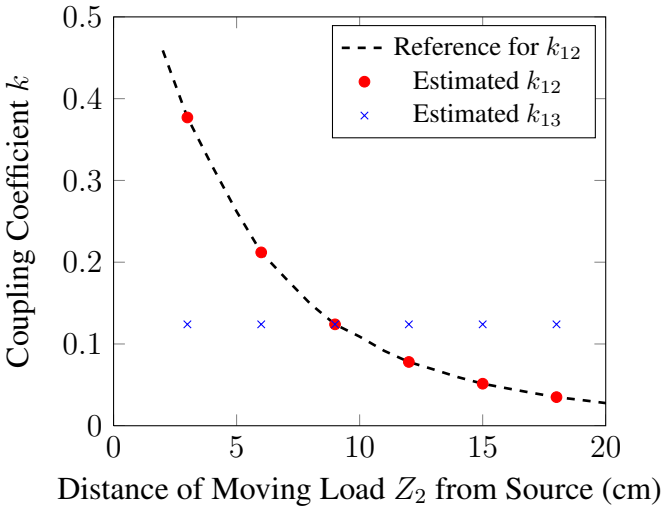

Figure 2.7: Simulation result for k_{12} and k_{13} estimation from transmitting side

transmitting frequency is fixed at 900 kHz. As mentioned in earlier section that by estimation from receiving side, only the k between itself and source can be obtained. Simulation results in Fig. 2.9 shows that estimated k value is consistent with the reference value regardless of the existence of an extra receiving antenna. The experimental shown in Fig. 2.10 is also mostly consistent with simulation result. The estimation errors occur in experiments at larger transmission gap is believed to be due to radiation loss. Note that, in contrast to k estimation result from the transmitting side, there are almost no error in estimation when transmitting gap is short when estimating k from the receiving side. Such difference is due to the fact that capacitance is not a parameter in k estimation equation from the receiving side.

Due to the fact that the estimation equation of coupling coefficient remains the same regardless of the number of receivers in the system, and that estimation value is much less affected by stray capacitance, k estimation equatioin from the receiving side is a promising approach for implementation of EV charging lane system. In the next chapter, the implementation of k estimation system from the receiving side will be discussed.

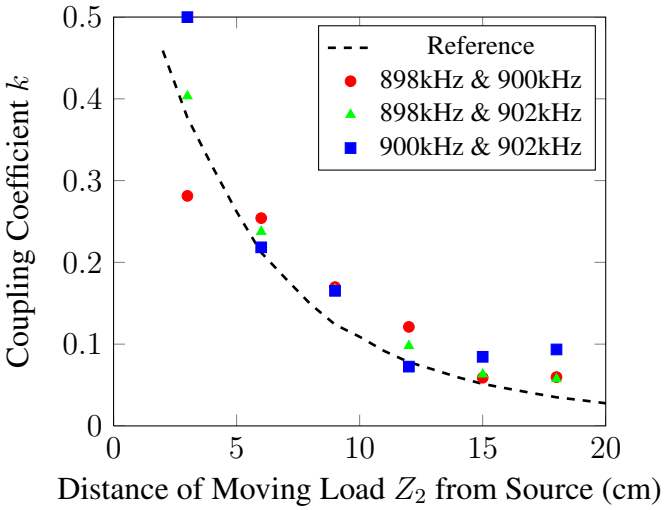

(a) k_{12} estimation result

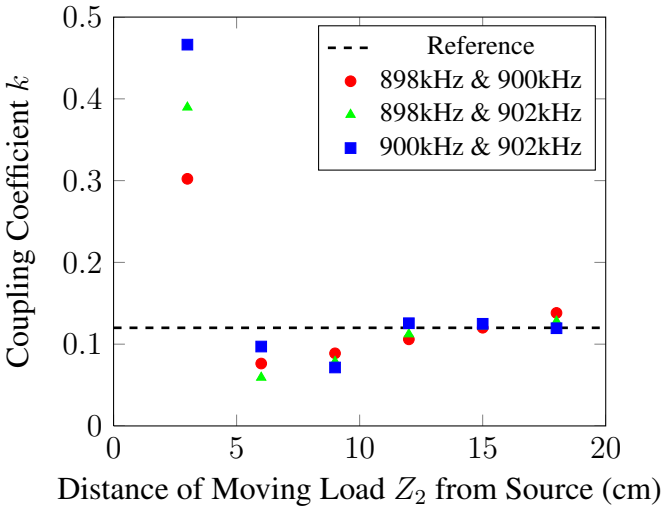

(b) k_{13} estimation result

Figure 2.8: Experiment result for k_{12} and k_{13} estimation from transmitting side using frequency sweep

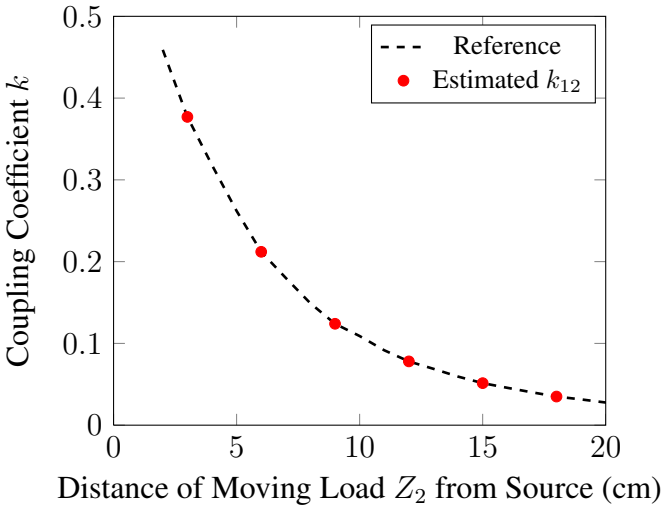

Figure 2.9: Simulation result for k_{12} estimation from receiving side

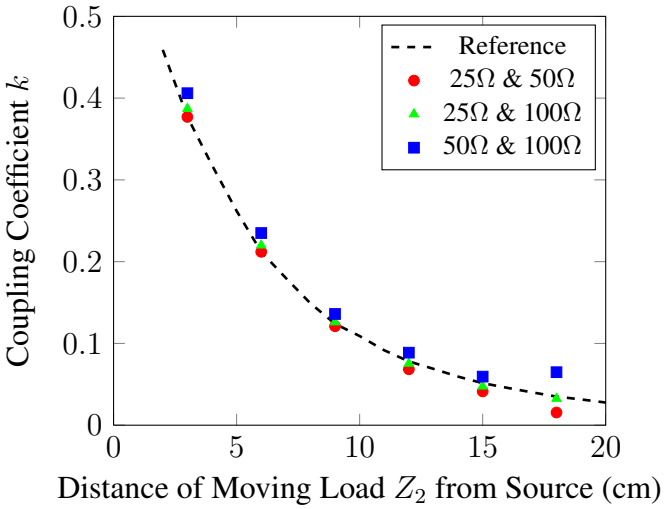

Figure 2.10: Experiment result for k_{12} estimation from receiving side using impedance sweep

Chapter 3

System Implementation using DC/DC

In actual application of efficient improving method, it is more practical to have load adjust its condition to match with source, especially when there are more than one receiver existing in the system. Also, as discussed in the previous chapter, among the proposed k estimation equation, the estimation equation from the receiving side remains simple regardless of the number of receivers in the system and is robust against stray capacitance, hence a promising k estimation approach. Therefore this study will focus on implementation of k estimator from the receiving side of wireless power transfer system.

As derived in the previous chapter, for k estimation from receiving side, necessary measurement is V_2 and controllable parameter is Z_2. In actual application, it is not possible to have users manually change load value of the vehicles. However, in terms of power electronics, DC/DC converter is a simple circuit that can achieve the task of changing voltage, hence change in load value. The possibility of using DC/DC to build k estimating system will be investigate in this chapter.

3.1 Concept of DC/DC Converter

DC/DC converter is a circuit that convert DC voltage source to another DC voltage. There are three types of switching mode DC/DC converters: buck, boost, and buck-boost con-

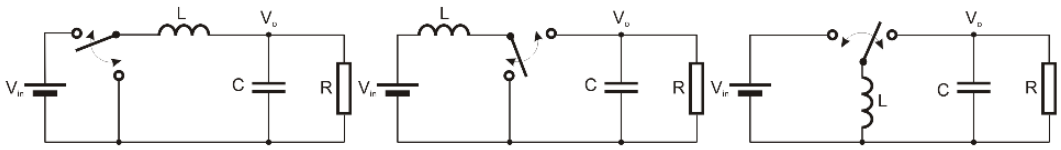

Figure 3.1: Schematics of Buck (left), Boost (middle), Buck-Boost (right) converters

Table 3.1: Comparison between Buck, Boost, Buck-Boost DC/DC Converter

Type	Voltage Ratio	Load Ratio	Range of Equivalent Load
Buck	$V_{out} = DV_{in}$	$Z_L = \frac{1}{D^2}R_L$	$R_L < Z_L < \infty$
Boost	$V_{out} = \frac{1}{1-D}V_{in}$	$Z_L = (1-D)^2 R_L$	$0 < Z_L < R_L$
Buck-Boost	$V_{out} = \frac{D}{1-D}V_{in}$	$Z_L = \frac{(1-D)^2}{D^2}R_L$	$0 < Z_L < \infty$

verters. Buck converter produces the output voltage that is lower than the input voltage, while boost converter produces the output voltage that is higher than the input voltage. Buck-boost converter can produce the output voltage either higher or lower than the source voltage. The simple structure of these DC/DC converters are illustrated in Figure 3.1. A comparison between the three types of converters are also shown in TABLE 3.1.

To enable load variation across broader range for estimation purpose, buck-boost converter is chosen for implementation of k estimating system.

3.2 System simulation in MATLAB/SimPowerSystem

3.2.1 Simulation Setup

The simulation of AC system for estimation from load side using DC/DC converter to sweep load impedance is conducted in MATLAB/Simulink. Load impedance is changed by adjusting duty cycle of the DC/DC converter. Simulink diagram is shown in Figure 3.2(a).

As mentioned in previous progress, for k estimation from receiving side, at least two sets of (V_2, Z_L) pair information are needed. In this section, estimation result using differ-

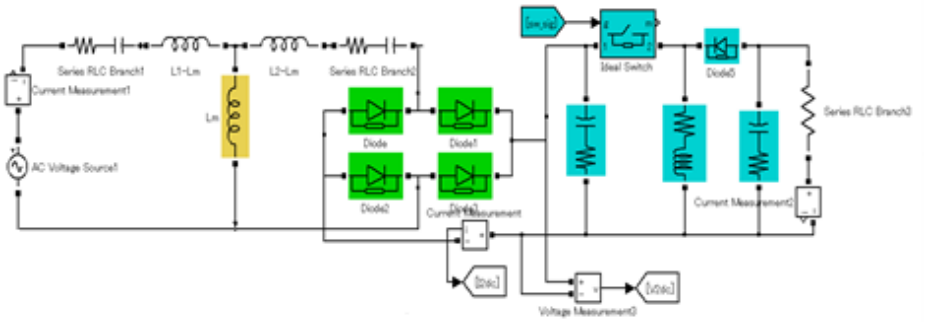

(a) Simulation setup for the case with 1 receiver

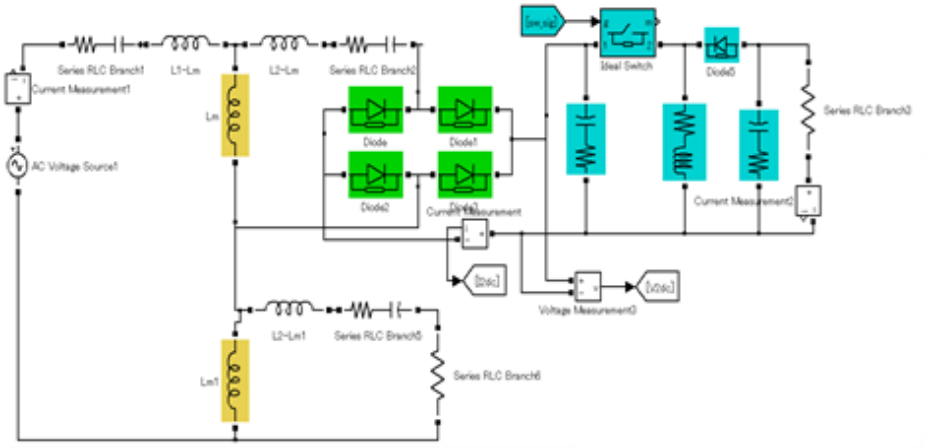

(b) Simulation setup for the case with 2 receivers

Figure 3.2: System Simulation in Simulink

ent pairs, one pair each time, is presented.

In this system, wireless power transfer system has resonant frequency of 900 kHz. The voltage on the receiving side, V_2 is passed through diode-bridge rectifier before being fed into buck-boost DC/DC converter. The duty cycle D of DC/DC converter is changed in order to change Z_L. For buck-boost converter, equivalent impedance Z'_L can be simply calculated by the relation $Z_L = 50\frac{(1-D)^2}{D^2}$, but in non-ideal system where there are losses in components, the efficiency of DC/DC converter will decrease, hence Z_L obtained by such equation will be significantly inaccurate. Therefore, in this system implementation load value will be calculated by $Z_L = \frac{V_2}{I_2}$. Duty cycle D is set to change every 2 ms. For each interval of the same D value, the estimator will wait for a certain amount of time, in this simulation for 1 ms, before reading V_2 value. Once two pairs of (V_2, Z_L) are obtained, the measured V_2 and the calculated Z'_L are then substituted into equation (2.10) to estimate coupling coefficient k. Since each pair of (V_2, Z_L) is corresponding with one duty cycle value, for simpler reference, from this point on the (V_2, Z_L) pair will be discussed in terms of duty cycle instead. Sample response of this system simulation is shown in Figure 3.3.

Simulations for multiple receivers are also setup as shown in Figure 3.2(b) for system with two receivers and similarly for system with three receivers.

3.2.2 Simulation Result

Following in Figure 3.4 are simulation results for estimation system using ideal buck-boost DC/DC converter. Each plain is the expected value of k for $k = 0.05 - 0.4$, and cross marks represent estimated value of k with respect to each pair of duty cycle. The ranged of duty cycle used in the simulation is chosen to be between 0.3 and 0.7 as it gives the range equivalent impedance of approximately between 10 Ω and 300 Ω.The results shows that estimated values match well with expected value of k. Hence, the feasibility of constructing estimation system using DC/DC converter is confirmed.

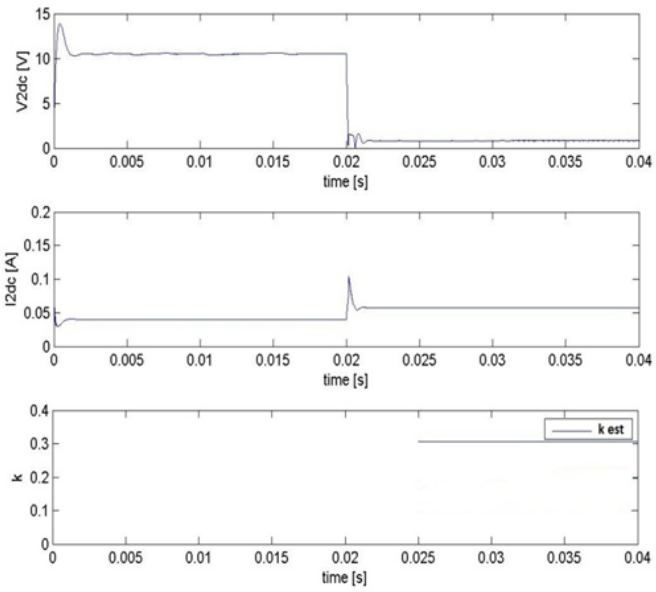

Figure 3.3: Response of system simulation when using D=0.3 and D=0.7 to estimate k_{12}

3.3 Experimental System

The system is realized using DC/DC converter. Controller, both for switching signal and for k estimation, is implemented using Arduino. System diagram is illustrated in Figure 3.5. The test system is first built on test board as shown in Figure 3.6. Estimation result for the case of system with one receiver and two receivers are shown in Figure 3.8(a) and Figure 3.8(b) respectively.

Estimation of coupling coefficient has been conducted with the constructed experimental system. Experimental setup is shown in Illustrated in Figure 3.7 to avoid cross coupling between different receivers. The distance of the antenna was set for when k is 0.1, 0.2 and 0.3. Results in this section shows calculation using direct measurement of V and I from the receiving side of the wireless power transfer system without any measurement filter.

Although the estimated values seem to be consistent regardless of which duty cycle pair is used for estimation, estimation results are significantly inaccurate. The reason for error estimation is believed to be due to non-ideal component in the system, which will be mentioned in the next section.

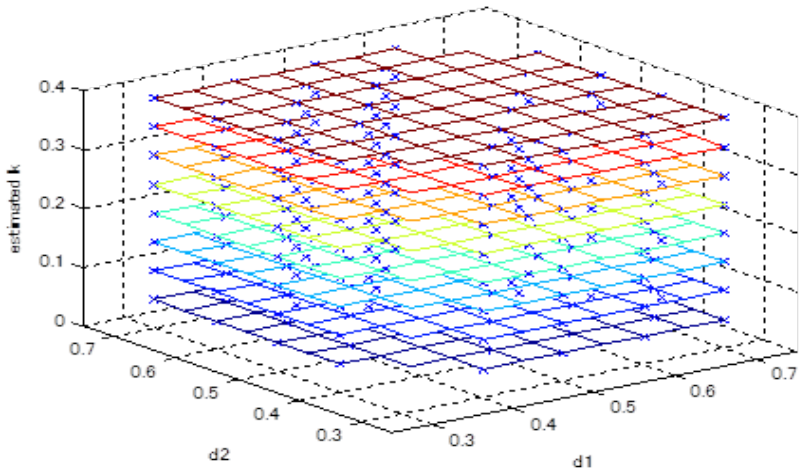

(a) k_{12} estimation result with single receiver

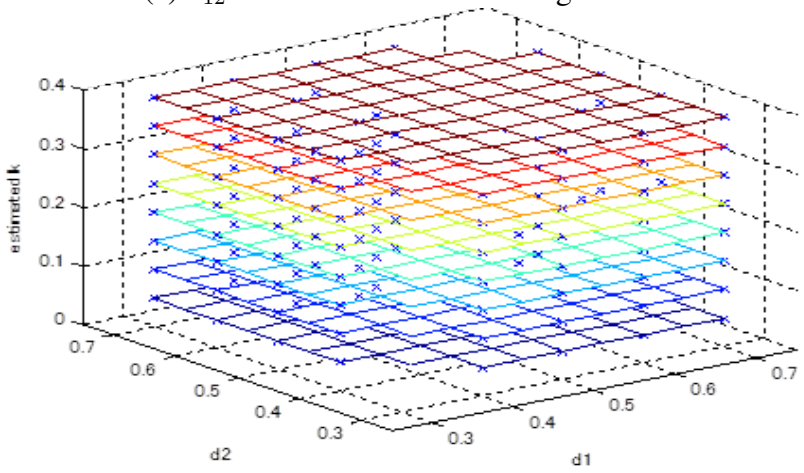

(b) k_{12} estimation result with 2 receivers

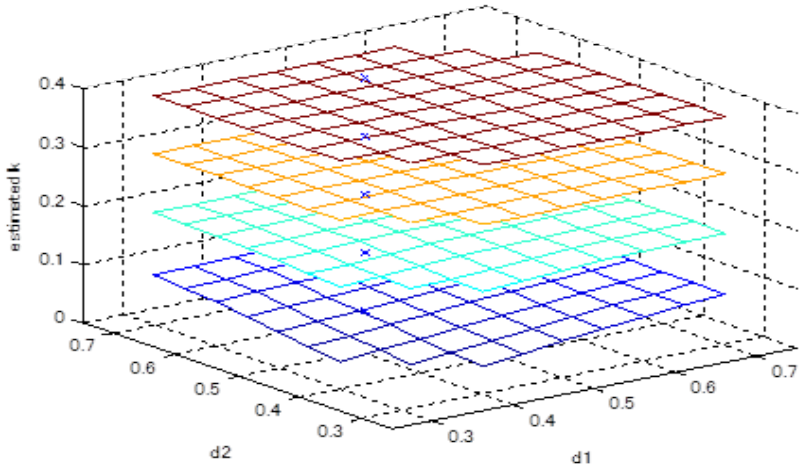

(c) k_{12} estimation result with 3 receivers

Figure 3.4: Simulation result of k estimation system using ideal DC/DC converter

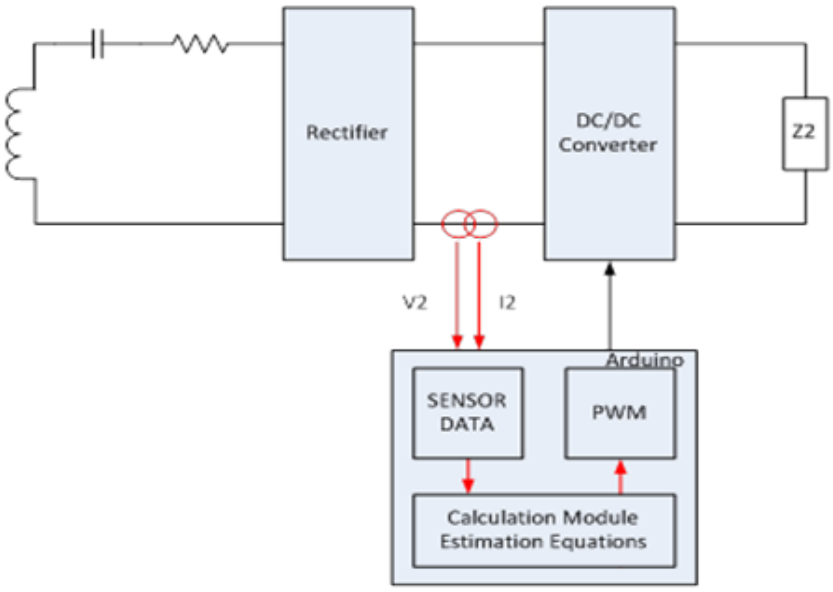

Figure 3.5: Experimental system diagram

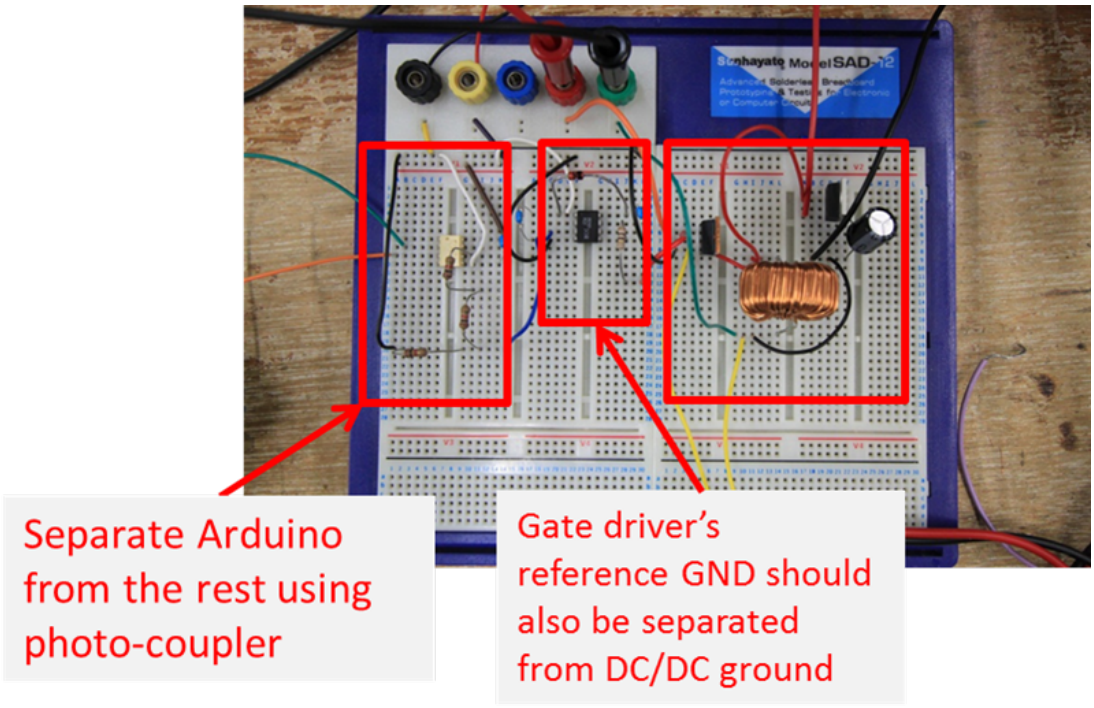

Figure 3.6: Experimental system built on test board

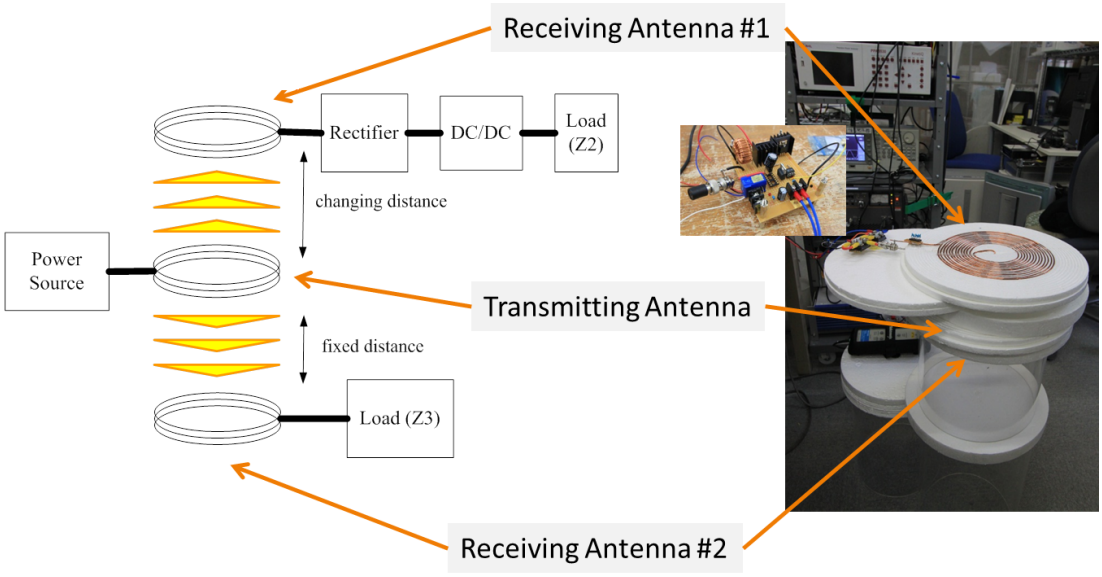

Figure 3.7: Experimental setup with k estimating system using DC/DC converter

Note that an experimental system for future experiment is also constructed. Receiving antenna with estimation system using DC/DC converter is placed onto the mobile robot as shown in Figure 3.9.

3.3.1 Possible Causes of Estimation Error

Diode Rectifier

Rectifier in this study is implemented using SiC diode for high frequency input. The output voltage from rectifier is expected to have voltage drop of approximately 2 times of the forward voltage of the diode (V_f). The measurement for when input voltage is from 1V to 10V shows the expected voltage drop as shown in Figure 3.10. Such voltage drop will also cause the change in equivalent impedance seen by the source, which is also one of the parameter in estimation equation.

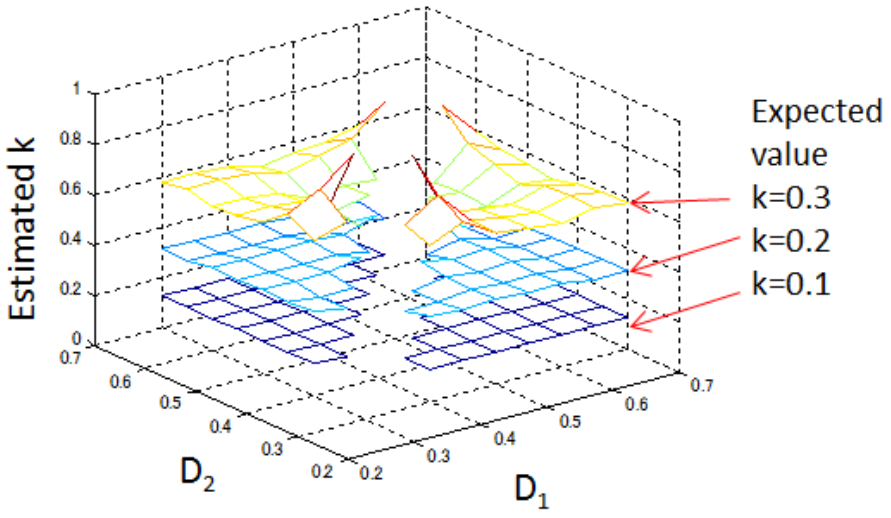

(a) k_{12} estimation result with single receiver

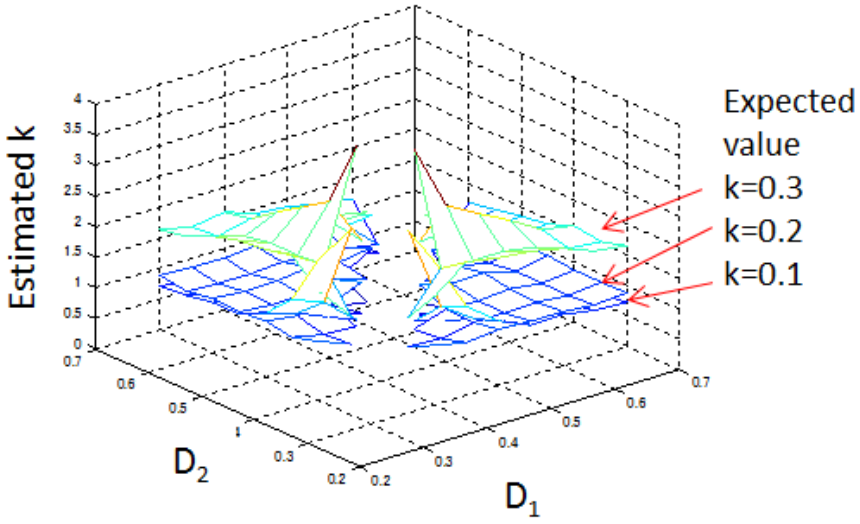

(b) k_{12} estimation result with 2 receivers

Figure 3.8: Experimental result of k estimation system using experimental system

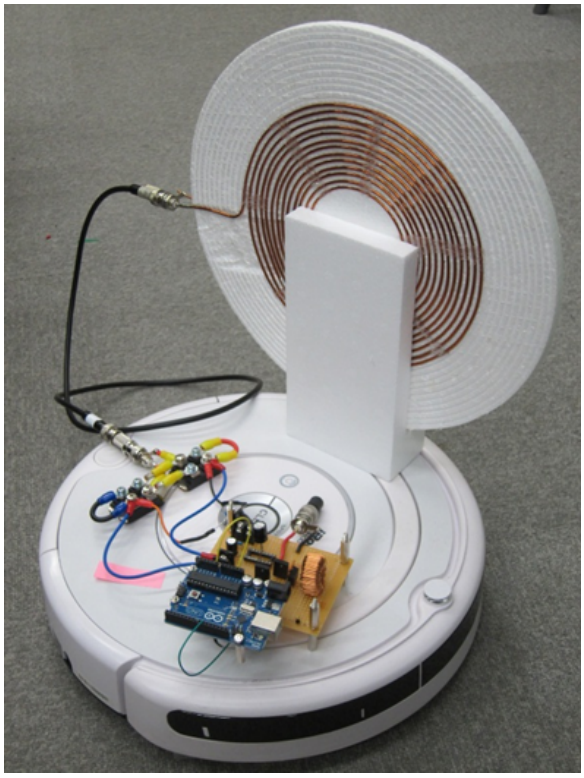

Figure 3.9: Experimental setup for moving load

DC/DC Converter

For functionality test of buck-boost converter, $\frac{V_{out}}{V_{in}}$ at different duty cycle is measured and calculated, when V_{in} and V_{out} are the input to and output from the DC/DC converter respectively. Up until now, ideal condition has been used for calculation; therefore the theoretical ratio of $\frac{V_{out}}{V_{in}}$ should be according to equation (3.1) where D is duty cycle.

$$\frac{V_{out}}{V_{in}} = \frac{D}{1-D} \tag{3.1}$$

However, the actual measurements for when V_{in} is from 1V to 10V show that the ratio tends to decrease when duty cycle is high. Such drop in voltage ratio is due to inductor's winding resistance R_L. By waveform analysis, the voltage ratio for non-ideal buck-boost converter can be expressed in equation (3.2). Figure 3.11 shows voltage ratio of ideal case, voltage ratio obtained from the actual measurement of experimental setup, and the

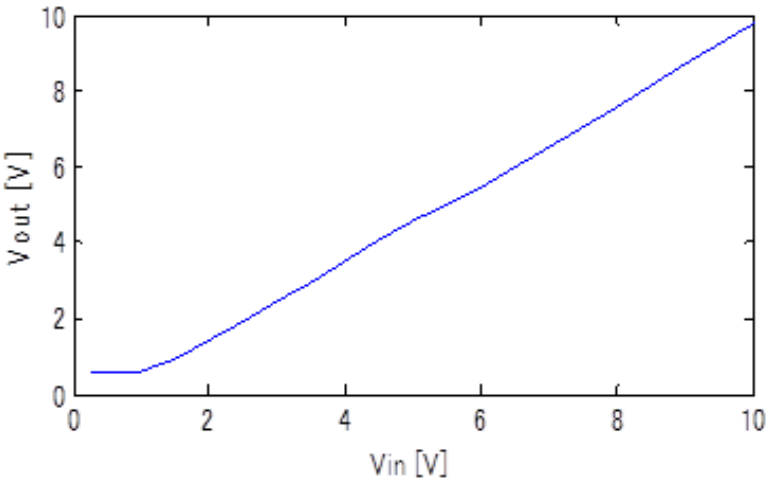

(a)Diode rectifier Ouput vs Input

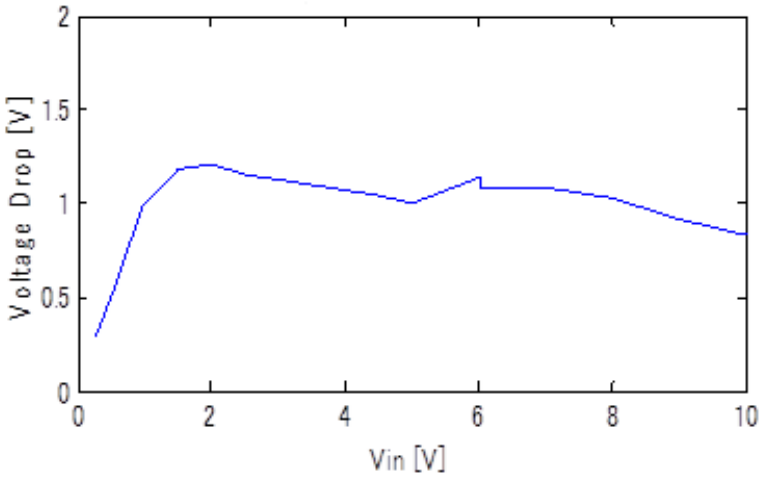

(b) Voltage drop in diode rectifier

Figure 3.10: Diode rectifier characteristics

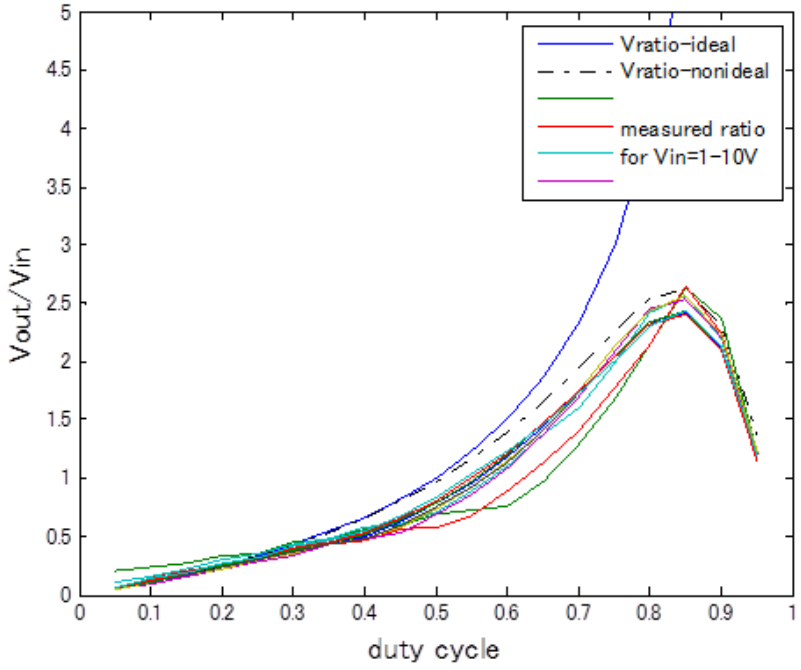

Figure 3.11: Buck-boost converter characteristics

calculated voltage ratio from non-ideal converter. The measurements is consistent with the case when R_L =1.8.

$$\frac{V_{out}}{V_{in}} = \frac{D}{1-D}\frac{1}{1+\frac{D^2 R_L}{(1-D)^2 R}} \tag{3.2}$$

However, such deterioration in efficiency should not cause deviation in relation between V_2 and Z_2 which is crucial to estimation equation.

Besides hardware imperfection, other possible cause for estimation error are measurement error. The next chapter will focus on method for reducing estimation error caused by such measurement error using least square approach.

Chapter 4

k Estimation Error Reduction using Recursive Least Square Method

Using measurement data directly in the k estimation equation presented in the previous chapter, there will be estimation errors due to either hardware imperfection or measurement noise as shown in Figure 4.1(a). If VNA is available, estimation system can be calibrated to give considerably much more accurate estimation result as shown in Figure 4.1(b). However, VNA is a rather expensive equipment, resulting in the fact that it is impractical to require every system to be equipped with it. Therefore, this study will be carried out with the assumption that VNA is not available for calibration.

4.1 Least Square Estimation

Least square method is a type of filter that is useful for system identification in noisy environment [27]. This method is effective in noise reduction when noise signal has zero average, therefore is appropriate for reduction of error caused by measurement error.

The standard form of this method is $y = Ax$ where y is desired response, A is a set of input samples and x is the parameter to estimate. In other words, y and A are known measurements and x is unknown parameter. Let $\hat{x}$ be the estimated value of x, estimation

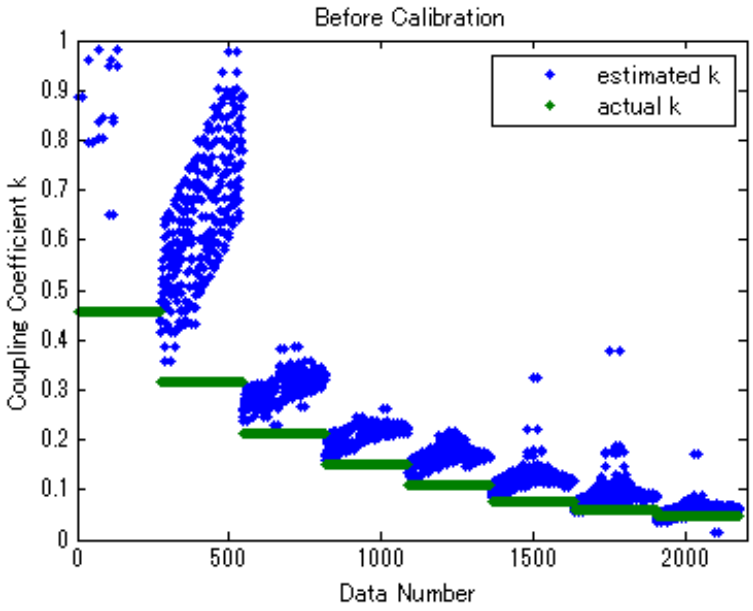

(a) Estimation result before calibration

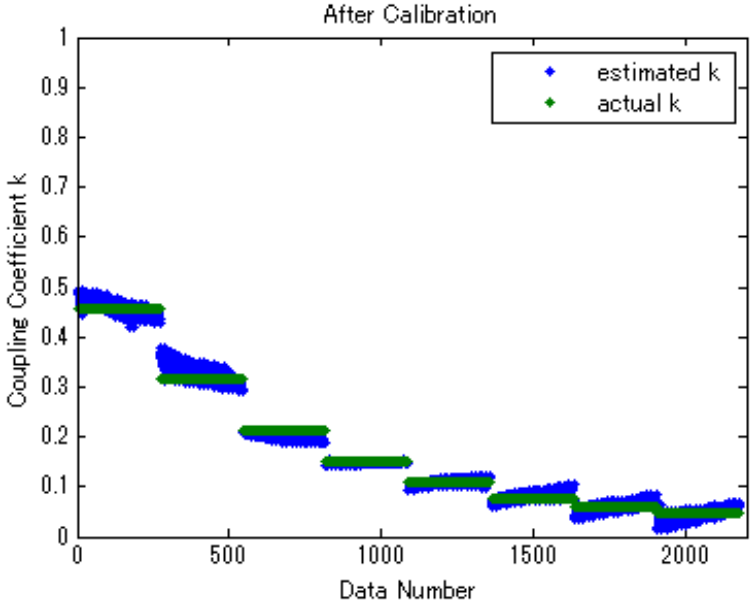

(a) Estimation result after calibration

Figure 4.1: k estimation result using VNA calibration

error is $\epsilon = y - A\hat{x}$. For least square estimation, cost function is defined as $J(\hat{x})$ in equation

4.1

$$\begin{aligned} J(\hat{x}) &= \epsilon^T \epsilon \\ &= (y - A\hat{x})^T (y - A\hat{x}) \\ &= y^T t - \hat{x}^T A y - y^T A \hat{x} + \hat{x}^T A^T A \hat{x} \end{aligned} \tag{4.1}$$

Cost function is minimized when $\frac{dj(\hat{x})}{d\hat{x}} = 0$, therefore $\hat{x}$ can be derived as shown in equation (4.2).

$$\begin{aligned} \frac{d(y^T y - \hat{x}^T A y - y^T A \hat{x} + \hat{x}^T A^T A \hat{x})}{d\hat{x}} &= 0 \\ -y^T A + \hat{x}^T A^T A &= 0 \\ \hat{x} &= (A^T A)^{-1} A^T y \end{aligned} \tag{4.2}$$

Although there is a standard form for least square estimation method, the way to define each parameter (A, x, y) is not unique. In this study, there are at least 2 ways to form the system equation into least square method standard form.

The first form, named form-1, is to express the system based on the estimation equation used in the previous chapter,

$$\begin{aligned} L_{12} &= \frac{V_1}{w} \frac{Z_{2a} V_{2b}(R_2 + Z_{2b}) - Z_{2b} V_{2a}(R_2 + Z_{2a})}{V_{2a} V_{2b}(Z_{2a} - Z_{2b})} \\ \frac{V_1}{w} \left(Z_{2a} V_{2b}(R_2 + Z_{2b}) - Z_{2b} V_{2a}(R_2 + Z_{2a})\right) &= V_{2a} V_{2b}(Z_{2a} - Z_{2b}) L_{12} \end{aligned} \tag{4.3}$$

In this case,

$$\begin{aligned} y &= \left[\tfrac{V_1}{w} \left(Z_{2a} V_{2b}(R_2 + Z_{2b}) - Z_{2b} V_{2a}(R_2 + Z_{2a})\right) \right] \\ A &= \left[V_{2a} V_{2b}(Z_{2a} - Z_{2b}) \right] \\ x &= \left[L_{12} \right] \end{aligned}$$

The second form, named form-2, is written based on the original equation of the wireless power transfer system before forming estimation equation. The information of other antenna which is unknown is also included in the equation, therefore such term is put into the matrix x as one of the parameters to estimate.

$$\frac{V_2}{V_1} = \frac{jwL_{12}\left(\frac{Z_2}{R_2+Z_2}\right)}{R_1+\frac{(\omega L_{12})^2}{R_2+Z_2}+\frac{(\omega L_{13})^2}{R_3+Z_3}+\dots}$$

Grouping terms for other antennas together into $Q = R_1+\frac{(\omega L_{13})^2}{R_3+Z_3}+\dots$

$$\begin{aligned}
\frac{V_2}{V_1} &= \frac{jwL_{12}\left(\frac{Z_2}{R_2+Z_2}\right)}{\frac{(\omega L_{12})^2}{R_2+Z_2}+Q} \\
\frac{V_2}{V_1}\left(\frac{(\omega L_{12})^2}{R_2+Z_2}+Q\right) &= jwL_{12}\left(\frac{Z_2}{R_2+Z_2}\right) \\
\frac{V_2}{V_1}\left(\frac{(\omega L_{12})}{R_2+Z_2}+Q'\right) &= \frac{Z_2}{R_2+Z_2} \\
\frac{Z_2}{R_2+Z_2} &= \begin{bmatrix}\frac{V_2}{V_1}\frac{\omega}{R_2+Z_2} & \frac{V_2}{V_1}\end{bmatrix}\begin{bmatrix}L_{12}\\ Q'\end{bmatrix}
\end{aligned} \tag{4.4}$$

In this case,

$$\begin{aligned}
y &= \begin{bmatrix}\frac{Z_2}{R_2+Z_2}\end{bmatrix} \\
A &= \begin{bmatrix}\frac{V_2}{V_1}\frac{\omega}{R_2+Z_2} & \frac{V_2}{V_1}\end{bmatrix} \\
x &= \begin{bmatrix}L_{12}\\ Q'\end{bmatrix}
\end{aligned}$$

Estimation results by least square method using form-1 and form-2 are shown in Figure 4.2 and Figure 4.3 for the system with one receiver and two receivers, respectively. For both forms, 2 ranges of training data were used, one is for when $D = 0.3-0.7$ and another

one is for when $D = 0.025 - 0.975$. Using least square method, estimation errors for the case when no filter was applied are shown to be reduced to some extent. The result for the case of single receivers in Figure 4.2 shows that, form-2 is more effective in reducing estimation error. The reason is believed to be that form-1 assumes that the other antennas' state including environment are unchanged during the estimation process while form-1 do no have such assumption. However, in the result for the system with two receivers in Figure 4.3, although estimation result by both forms are getting closer to the actual values of k, which form is more effective still needs further investigation by experiment with higher input power.

A weigting factor W may be assigned to emphasize relative importance amont the data observations. For this case, weighted error can be represented as $\epsilon = W(y - A\hat{x})$, hence, $\hat{x}$ that will minimize cost function is expressed in equation 4.5.

$$\hat{x} = (A^T W^T W A)^{-1} A^T W^T W y \tag{4.5}$$

4.2 Recursive Least Square

In case k is not always constant, recursive least square method is introduced in order to implement k estimation system with better accuracy.

Recursive Least Square is a type of adaptive filter algorithm which recursive finds the filter coefficients that minimize a weighted linear least squares cost function. The calculation is based directly on weighted least square estimation method, using forgetting factor as the weight to prioritize newer input signal data. A simple diagram of recursive least square method is illustrated in Figure 4.4.

Let λ be a forgetting factor and $0 \leq \lambda \leq 1$. A weight matrix W becomes as shown in equation (4.6).

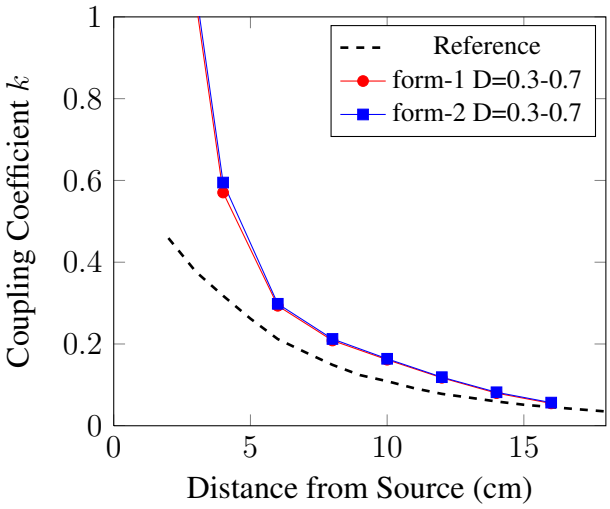

(a) with data from D=0.3-0.7

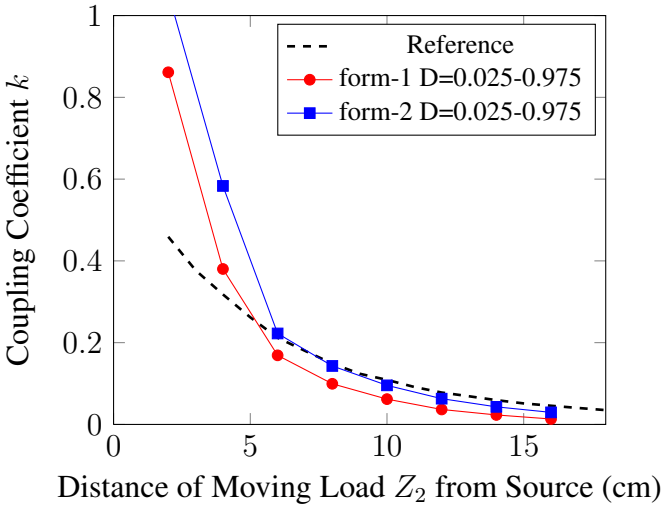

(b) with data from D=0.025-0.975

Figure 4.2: k estimation result with least square method for single receiver

$$W = \begin{bmatrix} 1 & 0 & 0 & \dots & 0 \\ 0 & \lambda & 0 & & \\ 0 & 0 & \lambda^2 & & \vdots \\ \vdots & & & \ddots & \\ 0 & & \dots & & \lambda^m \end{bmatrix} \tag{4.6}$$

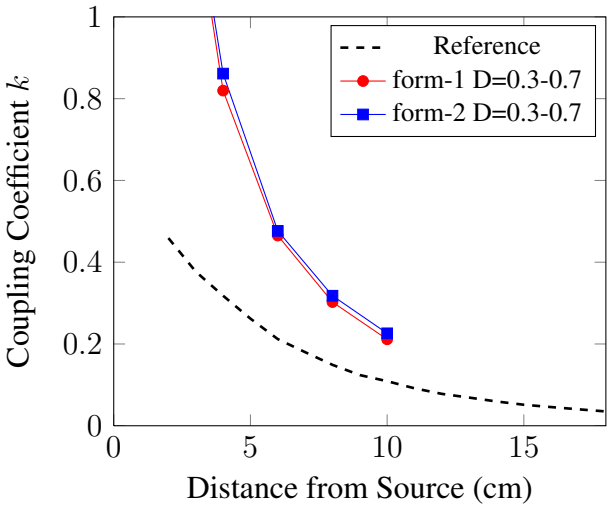

(a) with data from D=0.3-0.7

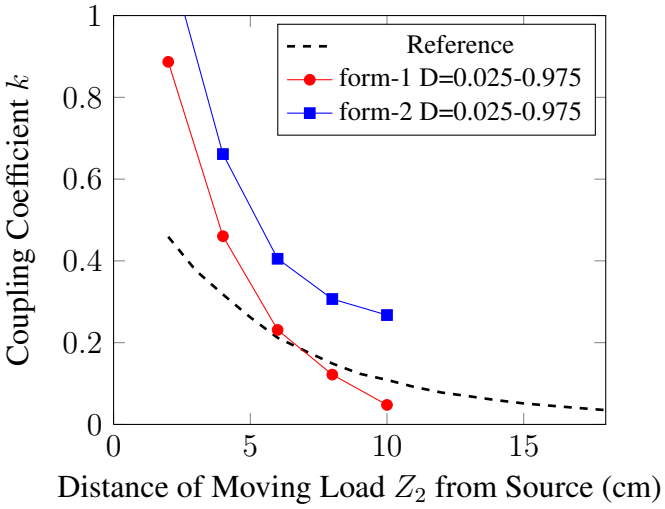

(b) with data from D=0.025-0.975

Figure 4.3: k estimation result with least square method for two receivers

where m = the number of measurement samples. If $\lambda = 1$, then all data is weighted equally. The typical value of λ is 0.98.

Estimation algorithm can be proceeded as follows.

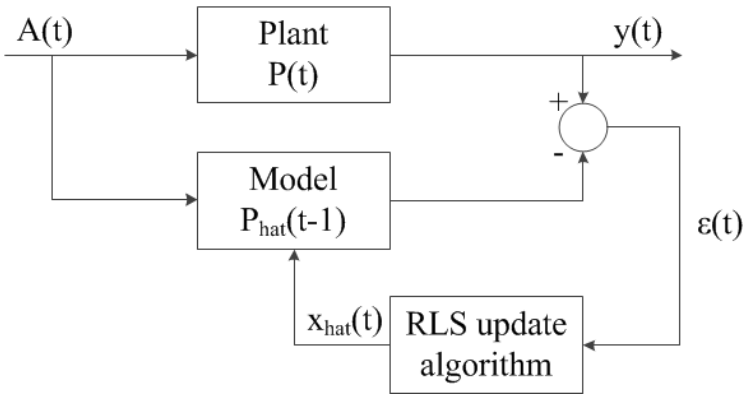

Figure 4.4: Block diagram of recursive least square method

1. Initialization

$$\hat{x}_0 = E(x) \tag{4.7}$$

$$P_0 = E((x - \hat{x}_0)(x - \hat{x}_0)\, T) \tag{4.8}$$

where $P =$ estimation-error covarience. If no prior knowledge of x is available, P_0 is initialized to $P_0 = \infty I$. In contrast, if perfect knowledge of x is available, then in the initialization step $P_0 = 0$.

2. Iteration

Based on the standard form $y = Ax$ and let i be the step number of estimation, estimator can be updated with new measurement as follows.

$$K_i = P_{i-1}A_i^T(A_iP_{i-1}A_i^T + R_i)^{-1} \tag{4.9}$$

$$\hat{x}_i = \hat{x}_{i-1} + K_i(y_i - A_i\hat{x}_{i-1}) \tag{4.10}$$

$$P_i = (I - K_iA_i)P_{i-1} \tag{4.11}$$

where $K =$ estimator gain.

By applying such procedure to system with time-varying k, measurement due to the current value of k will be prioritized rather than past values. The estimator coefficient is

constantly updated, and therefore should be efficient for k estimation method in the actual charging lane application.

In conclusion, although k estimation equation proposed in this study is valid theoretically, in practice there are still estimation errors due to imperfection of hardware and measurement error. By incorporating least square method into the estimation system, it is possible to obtain a much accurate estimation result of coupling coefficient.

Chapter 5

Conclusion

Summary

As a conclusion, a method for coupling coefficient k in wireless power transfer system via magnetic resonant coupling using only information from either the transmitting side or the receiving side of the system.

In Chapter 2, derivations of estimation equation are presented. It is possible to estimate coupling coefficient k, provided that all other antenna parameters are known, from either transmitting side or from receiving side of the system. Estimation can also be peformed regardless of the number of receivers existing in the system.

In Chapter3, as it is more practical to equip an efficiency improving system to the receiving side of wireless power transfer system, this study is focused on implementation of estimator from receiving side. The necessary measurement is voltage of the receiving side V_2 and the control parameter is load impedance Z_2. In order to automatically sweep Z_2 to get enough information needed for estimation, DC/DC converter is chosen as a mechanism to change Z_2. The system is implemented and experiment data are taken.

In Chapter 4, due to hardware imperfection and measurement noise, there are estimation error using experiment data. To reduce such estimation error, least square method is applied

to the system. Recursive least square method is also introduced as a potential method to improve estimation accuracy of k in case k is constantly changing as it would in charging lane application.

Future Topics

Although this study has derived relation equations for all case of estimation, both estimation from transmitting side and from receiving side for single receiver case and multiple receiver case, the implementation part has been focusing on estimation system from receiving side. There are still many opened topic regarding parameter estimation necessary for the realizaion of high efficiency EV charging lane. Possible future works include:

- Implementation of estimation system from transmitting side
- Study on the case with multiple transmitting antenna
- Simultaneous estimation of coupling coefficient and load resistance
- Effect of simultaneously control from both sides of the system

Appendix A

Effect of Obstacles to Power Transfer Efficiency

A.1 Effect from Mobile Robot

In order to use mobile robot for wireless power transfer experiment, it is necessary to investigate the effect of the mobile robot to the system to find the more appropriate setup. Power transfer efficiency due to each antenna configuration, with and without mobile robot is shown in Figure A.1.

The efficiency plots show that mobile robot has significant effect to power transfer if inserted in between transmitting antenna and receiving antenna. Therefore the appropriate setup for experimental setup is to have the mobile robot outside the two antennas. The possible configuration is shown in Figure A.2.

A.2 Effect from Bentonite

Wireless power transfer system also has potential application in the field such as nuclear power plant waste management. One crucial issue in operating nuclear power plant is nuclear waste management. The current method to handle the high-level nuclear waste is called Multi Barrier System, where nuclear waste is disposed deep underground within several layers of engineered and natural barriers. In order to demonstrate the safety condition within disposal system, the performance of Multi Barrier System will be confirmed by monitoring system. Therefore, various sensors are equipped inside the system for monitoring purpose. Until now, in order to obtain data from sensors, signal cables and power cords connected from sensors are drawn to the outside through small holes. To construct Multi Barrier System, the option of completely sealing the repository and having sensor data and power supply transmitted through wireless power transfer system has been proposed.

Wireless power transfer using magnetic resonance coupling method has been known to have the advantage of being able to transfer power across longer distance with considerably high efficiency and being robust to positional shift of transmitting antenna and receiving antenna. Repeater antennas can also be used to further extend the range of power transmission. Therefore, the mentioned wireless power transfer method is considered an

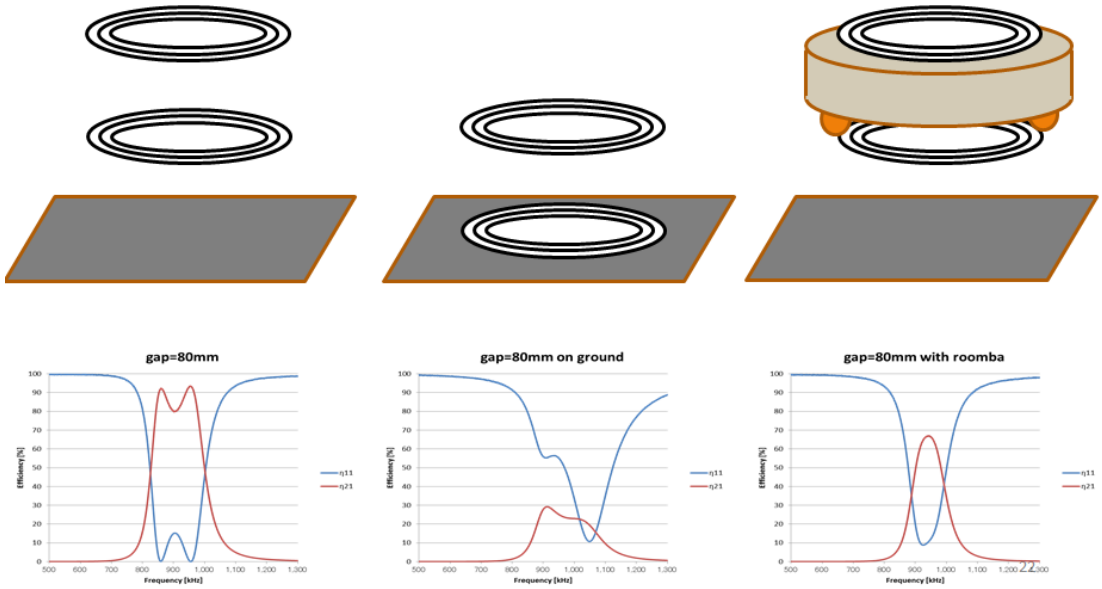

Figure A.1: Power transfer efficiency due to various configurations of experimental system

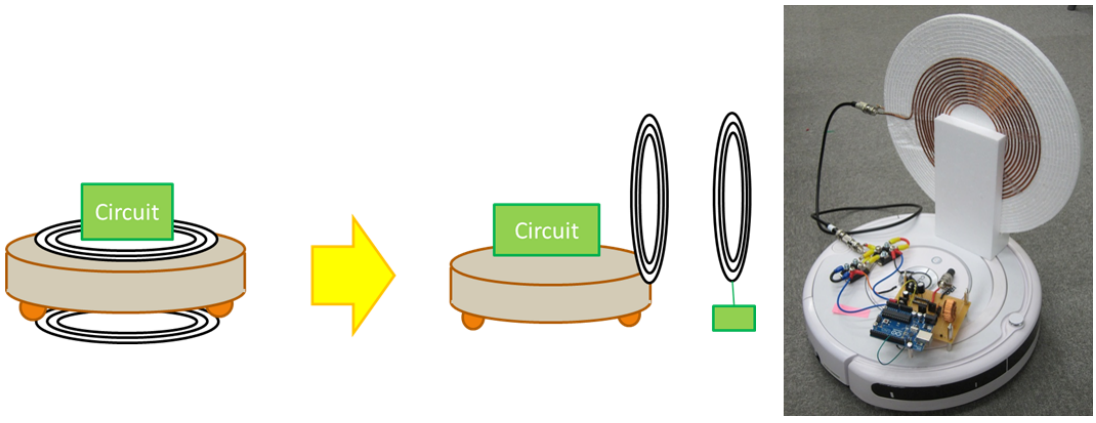

Figure A.2: One possible configuration for experimental setup to avoid effect from mobile robot

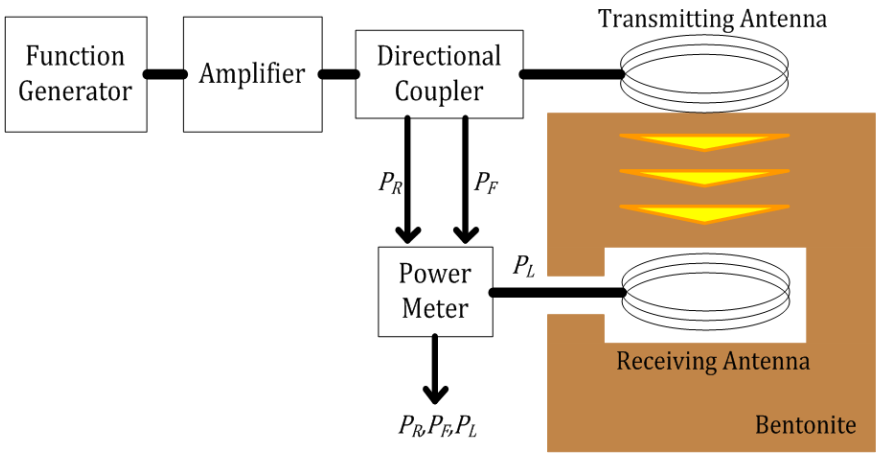

(a)Experimental configuration diagram

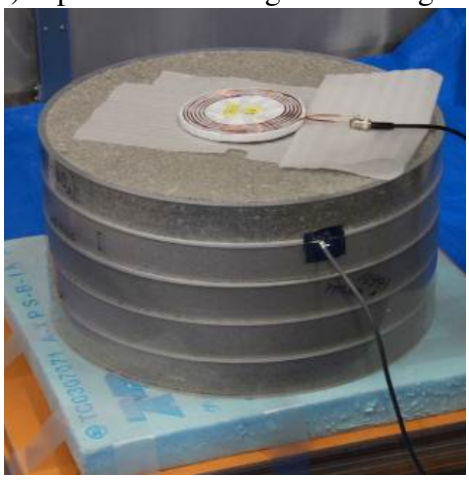

(b)Photo of experimental setup with bentonite

Figure A.3: Experimental setup with bentonite

attractive alternative for nuclear waste disposal monitoring system.Substance and material in between antennas such as soil and constructed containers are likely to have some effect on the efficiency of wireless power transfer system, and the possibility of power transfer being disrupted should also not be neglected. However, there have not been many studies available on such effect of substance and material to the wireless power transfer method.

Bentonite clay is a main component in natural barrier, due to its characteristics that it swells when exposed to water and becoming powerful barrier to water flow is utilized. Therefore, in this paper, bentonite clay is used for basis study on the effect of obstacle in wireless power transfer system. In the experiment, antennas of two different sizes are used and transmitting distance, or thickness of bentonite inserted between transmitting and receiving antennas, is varied. The efficiency of wireless power transmission with bentonite as barrier, with and without repeater antenna, is investigated and compared to the efficiency of wireless power transfer with no barrier material.

Experimental setup is shown in Figure A.3.

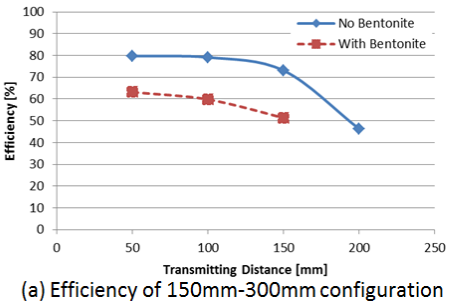

(a) Efficiency of 150mm-300mm configuration

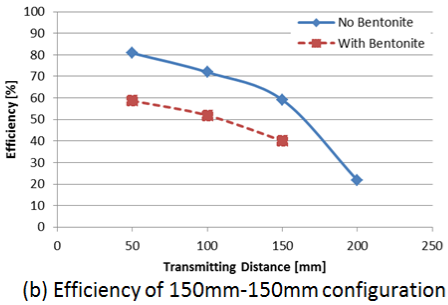

(b) Efficiency of 150mm-150mm configuration

Figure A.4: Efficiency comparison

For the configuration where transmitting antenna is 150 mm in diameter and receiving antenna is 300 mm in diameter or 150mm-300mm configuration, the efficiency after including bentonite block reduced to approximately 74.9% of the efficiency when transmitting power without bentonite. For the 150mm-150mm configuration, where both transmitting and receiving antenna are 150 mm in diameter, the efficiency with bentonite reduced to 70.8% of initial efficiency. The result plots are shown in Figure A.4

For the setup with repeater antenna, 150mm-150mm-150mm configuration with bentonite, overall efficiency is approximately 51%, and for 150mm-150mm-300mm configuration with bentonite block, overall efficiency is approximately 49%. The decreased efficiency is believed to be caused by 70-75% reduction in efficiency in each stage, according to data from section A of transmission efficiency by two antenna configuration.

Bibliography

[1] Kirsch, David A., "The Electric Car and the Burden of History: Studies in Automotiv Systems Rivalry in America". New Brunswick, New Jersey, and London: Rutgers University Press. pp. 153-162. ISBN 0-8135-2809-7.

[2] Hayes, J.G.; , "Battery charging systems for electric vehicles," Electric Vehicles - A Technology Roadmap for the Future (Digest No. 1998/262), IEE Colloquium on , vol., no., pp.4/1-4/8, 5 May 1998.

[3] Sunwin Bus http://www.sunwinbus.com/

[4] Joos, G.; de Freige, M.; Dubois, M.; , "Design and simulation of a fast charging station for PHEV/EV batteries," Electric Power and Energy Conference (EPEC), 2010 IEEE , vol., no., pp.1-5, 25-27 Aug. 2010

[5] Pei-Hsuan Cheng; Chern-Lin Chen; , "A high-efficiency fast charger for lead-acid batteries," IECON 02 [Industrial Electronics Society, IEEE 2002 28th Annual Conference of the] , vol.2, no., pp. 1410- 1415 vol.2, 5-8 Nov. 2002

[6] CHAdeMO Association http://www.chademo.com/

[7] Naoki Shinohara and Hiroshi Matsumoto, "Wireless Charging System by Microwave Power Transmission for Electric Motor Vehicles", IEICE vol.J87-C, no.5, p.433-443 (2004)

[8] Ronald J. Parise. "Future all-electric transportation communication and recharging via wireless power beam", Pro. SPIE 4214, 171 (2001).

[9] Selvakumaran, R.; Liu, W.; Soong, B.H.; Luo Ming; Loon, S.Y.; , "Design of inductive coil for wireless power transfer," Advanced Intelligent Mechatronics, 2009. AIM 2009. IEEE/ASME International Conference on , vol., no., pp.584-589, 14-17 July 2009

[10] Eghtesadi, M.; , "Inductive power transfer to an electric vehicle-analytical model ," Vehicular Technology Conference, 1990 IEEE 40th , vol., no., pp.100-104, 6-9 May 1990

[11] Sungwoo Lee; Jin Huh; Changbyung Park; Nam-Sup Choi; Gyu-Hyeoung Cho; Chun-Taek Rim; , "On-Line Electric Vehicle using inductive power transfer system,"Energy Conversion Congress and Exposition (ECCE), 2010 IEEE , vol., no., pp.1598-1601, 12-16 Sept. 2010

[12] Andre Kurs, Aristeidis Karalis, Robert Moffatt, J.D. Joannopoulos, Peter Fisher, Marin Soljacic, "Wireless Power Transfer vis Strongly Coupled Magnetic Resonances," in Science Express on 7 June 2007, vol.317, no.5834, p.83-86.

[13] Junhua Wang; Ho, S.L.; Fu, W.N.; Mingui Sun; , "A comparative study between witricity and traditional inductive coupling in wireless energy transmission," Electromagnetic Field Computation (CEFC), 2010 14th Biennial IEEE Conference on , vol., no., pp.1, 9-12 May 2010

[14] Takehiro Imura, Toshiyuki Uchida, Yoichi Hori, "Flexibility of Contactless Power Transfer using Magnetic Resonance Coupling to Air Gap and Misalignment for EV", IEEE Electric Vehicle driven on Electric Vehicle Symposium 24, 2009.5

[15] Teck Chuan Beh; Imura, T.; Kato, M.; Hori, Y.; , "Basic study of improving efficiency of wireless power transfer via magnetic resonance coupling based on impedance matching," Industrial Electronics (ISIE), 2010 IEEE International Symposium on , vol., no., pp.2011-2016, 4-7 July 2010

[16] Wenzhen Fu; Bo Zhang; Dongyuan Qiu; , "Study on frequency-tracking wireless power transfer system by resonant coupling," Power Electronics and Motion Control Conference, 2009. IPEMC '09. IEEE 6th International , vol., no., pp.2658-2663, 17-20 May 2009

[17] Yukiko Yokoi, Akihiko Taniya, Masaki Horiuchi and Shigeru Kobayashi, "Development of kW class wireless power transmission system for EV using magnetic resonant method", EVTeC'11.

[18] Hanazawa, M.; Ohira, T.; , "Power transfer for a running automobile, "Microwave Workshop Series on Innovative Wireless Power Transmission: Technologies, Systems, and Applications (IMWS), 2011 IEEE MTT-S International , vol., no., pp.77-80, 12-13 May 2011

[19] K. Onizuka, et al, "Coupling factor estimation for efficiency optimization on wireless power transfer,"2010 IEICE General Conference, Proceedings B. B-1-29, pp.29, Mar 2010

[20] Nakamura, S.; Ajisaka, S.; Koma, R.; , "Pinpoint Wireless Power Transformation System using Reflection Coefficient in Magnetic Resonance Coupling," 7th International Conference on Ubiquitous Robots and Ambient Intelligence, 2010

[21] Thrimawithana, D.J.; Madawala, U.K.; , "A primary side controller for inductive power transfer systems," Industrial Technology (ICIT), 2010 IEEE International Conference on , vol., no., pp.661-666, 14-17 Mar 2010

[22] Beh Teck Chuan, "Basic Research on Wireless Power Transfer System via Magnetic Resonant Coupling at MHz Range - Efficiency Improvement Based on Impedance Matching, " Undergraduate Thesis, The University of Tokyo, Feb 2010

[23] Takehiro Imura, Hiroyuki Okabe, Toshiyuki Uchida, Yoichi Hori, "Study on Open and Short End Helical Antennas with Capacitor in Series of Wireless Power Transfer using Magnetic Resonant Couplings", IEEE Industrial Electronics Society Annual Conference, 2009.11

[24] Koh Kim Ean; Beh Teck Chuan; Imura, T.; Hori, Y.; , "Novel bandpass filter model for multi-receiver wireless power transfer via magnetic resonance coupling and power division, "Wireless and Microwave Technology Conference (WAMICON), 2012 IEEE 13th Annual, pp.1-6, 15-17 April 2012

[25] Chwei-Sen Wang; Stielau, O.H.; Covic, G.A.; , "Design considerations for a contactless electric vehicle battery charger," Industrial Electronics, IEEE Transactions on, vol.52, no.5, pp. 1308-1314, Oct 2005

[26] Yusuke Moriwaki, Takehiro Imura, Yoichi Hori. "Basic Study on Reduction of Reflected Power Using DC/DC Converters in Wireless Powre Transfer System via Magnetic Resonant Coupling," INTELEC, Oct 2011

[27] Ad Van Den Boom. System Identification, on the variety and coherence in parameter- and order estimation methods. Technische Hogeschool Eindhoven, 1982

Publications

- Vissuta Jiwariyavej, Takehiro Imura, Yoichi Hori, "Coupling Coefficients Estimation of Wireless Power Transfer System via Magnetic Resonance Coupling using Information from Either Side of the System," in Proc. the 2012 International Conference on Broadband and Biomedical Communication (IB2COM 2012), Sydney, Australia, Nov 2012

- Vissuta Jiwariyavej, Takehiro Imura, Takuya Koyanagi, Yusuke Moriwaki, Yoichi Hori, Chiaki Nagai, Kenichi Ando, Kazuya Watanabe, Masao Uyama, "Basic Experimental Study on Effect of Bentonite to Efficiency of Wireless Power Transfer Using Magnetic Resonance Coupling Method," in Proc. 33rd International Telecoommunications Energy Conference (INTELEC 2011), Amsterdam, Netherlands, 2011

- Masahiko Tsuboka, Vissuta Jiwariyavej, Takehiro Imura, Hiroshi Fujimoto, Yoichi Hori, "Secondary Parameter Estimation for Wireless Power Transfer System Using Magnetic Resonance Coupling," IEE of Japan Technical Meeting Record, pp. 77-80, 2012 (in Japanese)

Acknowledgements

First of all, I would like to thank Professor Yoichi Hori, Professor Hiroshi Fujimoto, and Dr. Imura for valuable guidances throughout my three years in this laboratory. I have learnt a lot not only about electrical engineering but also received many good life advice.

I would also like to thank members of wireless team for all the things you taught me and all your support especially when I'm stuck with problems. Thank you Hori-Fujimoto lab members as you are like my family that are always there for me and making my life here very lively.

Thank from the bottom of my heart to my parents and family who always watch over me even from overseas. I wouldn't be able to reach here without you. Last but not least, to all my friends who are always all ears and cheer me up, let me tell you that your cheers have helped me get through many tough days.